5-24-2018

Predictive Data-Based Multi-Hazard Hurricane Fragility Models for Single Family Homes

Carol Constantin Massarra
Louisiana State University and Agricultural and Mechanical College, cmassa1@lsu.edu

PREDICTIVE DATA-BASED MULTI-HAZARD HURRICANE FRAGILITY MODELS FOR SINGLE FAMILY HOMES

A Dissertation

Submitted to the Graduate Faculty of the
Louisiana State University and
Agricultural and Mechanical College
in partial fulfillment of the
requirements for the degree of
Doctor of Philosophy

in

The Interdepartmental Program in Engineering Science

by
Carol Constantin Massarra
B.C.E., Tishreen University, 1999
M.S., Louisiana State University, 2012
M.Ap.Stat., Louisiana State University, 2016
August 2018

My mother, I love you more than anything else.

Daddy, I trust you are there watching me. I miss you today and every day.

ACKNOWLEDGEMENTS

I would like to thank my committee members collectively and individually: Carol Friedland, Brian Marx, Steve Cai, and Michael Leitner. They have been instrumental in my graduate education through coursework and helping guide my research at Louisiana State University. I am grateful to Shandy Ogea Heil and Elizabeth Matthews for being my best friends. I gratefully acknowledge funding for this research from the Louisiana Board of Regents Graduate Fellowship in Engineering Grant # LEQSF(2008-13)GF-01, the Donald W. Clayton Graduate PhD Assistantship in Engineering, the Chevron Engineering Graduate Student Fellowship, and the Bert S. Turner Department of Construction Management at LSU. Hurricane Katrina reconnaissance videos were provided by MCEER (http://www.buffalo.edu/mceer.html). I am thankful to Dr. Casey Dietrich from North Carolina State University for providing the hazard data. I am thankful to my two brothers who have always been there for me when I needed support. Last but not least, I am forever thankful to my mother for being my smile throughout my life.

TABLE OF CONTENTS

LIST OF TABLES

LIST OF FIGURES

ABSTRACT

Recently, data-based fragility models have been implemented to explain multi-hazard hurricane building fragility. However, deficiencies in current fragility models exist. Typically, categorical dependent variables are modeled as continuous numerical variables, which may result in inefficient standard errors for estimated coefficients and the models may result in probabilities greater than one or less than zero. Additionally, published models are limited to inference and interpretation of main variable coefficients without consideration of interaction terms between the variables and do not consider evaluation of model performance.

This dissertation addresses these deficiencies in the development of predictive data-based fragility models for multinomial categorical damage states (DS) and binary collapse/non-collapse using proportional odds cumulative logit and logistic regression models, respectively. The models are fitted as a function of hazard parameters and their interactions (Chapter 2) and as a function of hazard parameters, building attributes, and their interactions (Chapter 4). Chapter 3 develops numerical imputation diagnostic and comparison approaches for missing binary data, providing a methodology to evaluate imputation techniques that maximize field reconnaissance data for integration in Chapter 4. Fragility model prediction accuracy is evaluated using "leave-one-out" cross-validation (LOOCV), expressed in terms of the cross-classification rate (CCR). Model inputs are physical damage and building attribute data collected in coastal Mississippi following 2005 Hurricane Katrina and high-resolution, numerical hindcast hazard intensities from the Simulating Waves Nearshore and ADvanced CIRCulation (SWAN+ADCIRC) models.

For models excluding building attributes, maximum significant wave height is a significant DS predictor, while maximum 3-second gust wind speed, maximum surge depth, and maximum water speed are significant collapse predictors. Model prediction accuracy ranges from 81% to 87%. For models including building attributes, maximum 3-second gust wind speed, maximum

significant wave height, maximum water speed, foundation type, number of stories, and the interaction of both maximum water speed and maximum significant wave height with number of stories are significant DS predictors. Building attributes, maximum surge depth above local ground, maximum water speed, maximum significant wave height, foundation type, number of stories, and the interaction of maximum significant wave height with number of stories are significant collapse predictors. Model prediction accuracy ranges from 84% to 90%.

CHAPTER 1. INTRODUCTION

Buildings are vulnerable to damage from multiple, sequential, and simultaneous hurricane hazards. Wind events and combined wind and flood events (e.g., hurricanes) have caused 90% of the total insured losses in the U.S. in the last twenty years (Katz, 2013). The damage generated by multi-hazard events may be greater than the aggregation of damage caused by each hazard separately (Kappes et al., 2012a; Kappes et al., 2012b), so development of methods that explicitly consider combined hazards are needed across science and engineering. Historically, residential construction has been disproportionately affected by hurricanes in the U.S. because approximately 90% of residential buildings are light frame, non-engineered wood construction (Ellingwood et al., 2004; Grayson et al., 2013). Traditionally, damage models relate a single hazard intensity (e.g., wind speed, inundation depth) to physical damage, and are developed through mechanics-based analysis and stochastic simulation techniques. By modeling an individual building or an array of buildings through parametric modeling, building response as a result of increasing hazard load is documented in the form of a fragility functions, which represent the probability of collapse or being in or exceeding a specified damage state as a function of one hazard intensity. These functions are highly dependent upon structural and hazard characteristics, as well as the probabilistic parameters selected to represent uncertainty.

For the multi-hazard hurricane environment, research has primarily focused on simulation for modeling building vulnerability (e.g., Barbato et al., 2013; Choine et al., 2015; Lee & Rosowsky, 2006; Li & Ellingwood, 2009a, 2009b; Li & van de Lindt, 2012; Li et al., 2011; Liu et al., 2015; Pan, 2014; Schmidt et al., 2011). However, these models are not yet capable of representing the physical, temporal, and spatial variability of a population of buildings subjected to an event-specific hazard sequence across a spatial domain. Under multi-hazard conditions, simulation of a building's behavior and the combined effects between multiple hazards and

building response become very complex (van Verseveld et al., 2015) or even impossible to accurately model (Marzocchi et al., 2012). Difficulties stem from disparate and temporal hazard characteristics (Kappes et al., 2012a; Kappes et al., 2012b), and the wide variety of building configurations (Ellingwood et al., 2004).

Data-based multi-hazard hurricane fragility models have recently been used to model building damage as a function of hazard parameters and environmental and building attributes (e.g., Hatzikyriakou & Lin, 2018; Hatzikyriakou et al., 2015; Tomiczek et al., 2014b; Tomiczek et al., 2017). Data-based models have also been used to model building damage from tsunami hazards (Charvet et al., 2014a; Charvet et al., 2014b; Charvet et al., 2015; Reese et al., 2011) and earthquake hazards (Lallemant et al., 2015). Although not specific to buildings, data-based models have been used to model fragility of power systems (Reed et al., 2016) and oil storage tanks (Kameshwar & Padgett, 2018) for hurricane hazards.

Given the issues in simulation-based models and the increasing acknowledgment of the need to better predict outcomes for multi-hazard scenarios (Barbato et al., 2013; Friedland & Gall, 2012; Kappes et al., 2012b; Li et al., 2011; McCullough et al., 2013), models other than simulation-based models are needed to address the multi-hazard hurricane complexities and represent multiple predictor variables. Data-based models offer a viable solution, as observed data are used for model fitting; therefore, these models inherently account for aspects such as location effects and variability in building and environmental attributes (Pitilakis et al., 2014). Evaluating the prediction accuracy of data-based models using external cross-validation (CV), also reliant on observed data, is an advantage over simulation-based fragility models. Data-based models do not suffer from issues encountered in quantification of simulation-based model prediction accuracy that results from the lack of observed data (Baradaranshoraka et al., 2017; Ellingwood et al., 2004).

The aforementioned characteristics of data-based models are of particular value for non-engineered or marginally engineered buildings (e.g., single family houses), where building parameters may not be available or not practical to model for individual buildings.

Data-based multi-hazard hurricane fragility models have recently been used to model building damage as a function of hazard parameters and environmental and building attributes (e.g., Hatzikyriakou & Lin, 2018; Hatzikyriakou et al., 2015; Tomiczek et al., 2014b; Tomiczek et al., 2017). Data-based models have also been used to model building damage from tsunami hazards (Charvet et al., 2014a; Charvet et al., 2014b; Charvet et al., 2015; Reese et al., 2011) and earthquake hazards (Lallemant et al., 2015). Although not specific to buildings, data-based models have been used to model fragility of power systems (Reed et al., 2016) and oil storage tanks (Kameshwar & Padgett, 2018) for hurricane hazards.

Two primary types of data-based fragility models emerge from the literature – those considering only hazard attributes (e.g., Charvet et al., 2014a; Charvet et al., 2014b; Reed et al., 2016) and those considering both hazard and building attributes (e.g., Hatzikyriakou & Lin, 2018; Tomiczek et al., 2014a; Tomiczek et al., 2017). Models that consider only hazard parameters are useful when detailed information about study area buildings is not available (e.g., quick planning exercises, pre-event forecasting), while models that consider both hazard and building attributes provide greater detail about the performance of buildings based on damage indicator variables. These models are appropriate when detailed inventory data are available.

Within residential data-based hurricane fragility modeling literature, dependent variables are treated either as multinomial categorical ordered damage states (e.g., Hatzikyriakou & Lin, 2018; Tomiczek et al., 2017) or as binomial collapse/non-collapse (e.g., Hatzikyriakou et al., 2015; Tomiczek et al., 2014a), while the explanatory variables are combinations of hazard parameters

and environmental and building attributes. In published models (e.g., Hatzikyriakou et al., 2015; Tomiczek et al., 2014a; Tomiczek et al., 2017), the main focus is on inference and interpretation of model coefficients without evaluation of model performance. While inference and interpretation provide insight on the effect of explanatory variables on damage, external validation is needed to evaluate model performance, thus providing a realistic evaluation of model prediction accuracy for future events. In existing literature, interactions between hazard parameters and building attributes are rarely modeled, and the majority of models are fitted as a function of main effects only (i.e., hazard variables and/or environmental and building attributes) (e.g., Hatzikyriakou & Lin, 2018; Hatzikyriakou et al., 2015; Tomiczek et al., 2014a). Tomiczek et al. (2017) evaluated interaction between hazard parameters and building attributes but without inference and interpretation of the interaction coefficients. When hazard parameter and building attribute interaction terms are statistically significant, this indicates that the effect of hazard on damage varies across the levels of building attributes; therefore, damage prediction and inference must be based on both main and interaction terms. Additionally, categorical dependent variables have been modeled as continuous numerical variables (e.g., Tomiczek et al., 2014a; Tomiczek et al., 2017), which may result in probabilities greater than one or less than zero, and can have inefficient standard errors for the estimated coefficients because the discrete nature of the response is not modelled.

Missing data is common issue for the data-based models. Particularly for data-based models that consider hazard and building attributes, building attribute data may not be fully observed. Given the large number of destroyed buildings after a hurricane event, the common practice of imputation is applied to estimate missing observation data, maximizing the usefulness of the observed data. When building attributes are described by binary categorical variables (e.g., one-story, two-story),

logistic regression model-based imputation techniques are widely used (Berglund & Heeringa, 2014). Although these techniques are well developed to impute missing observations for categorical variables, approaches to diagnose and compare the imputation models resulting from these techniques are lacking. Current numerical diagnostic approaches are limited to imputation models for continuous variables (e.g., Abayomi et al., 2008; Farhan & Fwa, 2014; Stuart et al., 2009; Van Buuren, 2012; White et al., 2011; Zhu et al., 2009), while comparison approaches are limited to evaluation of the performance of the statistical models fit on the imputed dataset rather than on the imputation models themselves (e.g., Akande et al., 2017; Collins et al., 2001; Raghunathan et al., 2001).

1.1 Problem Statement

Although some studies address data-based modeling of multi-hazard hurricane damage, several challenges remain. Deficiencies in published models include 1) inappropriate use of modeling approaches for multinomial and binomial responses, 2) lack of consideration and interpretation of interaction terms, especially between hazard parameters and building attributes, 3) absence of model performance evaluation for future damage prediction, and 4) absence of numerical diagnostic and comparison approaches for binary variable imputation models.

1.2 Goal and Objectives

The underlying goal of this dissertation is to improve data-based damage prediction for residential construction subjected to multi-hazard hurricane hazards at the individual building scale. As a step towards achieving this goal, three objectives are undertaken:

- Develop predictive data-based hurricane building (i.e., global) fragility models as functions of hurricane hazard parameters and their interactions.

- Develop diagnostic and comparison approaches to evaluate the performance of binary variable imputation models used to maximize use of aftermath datasets with missing building attribute data.
- Develop predictive data-based hurricane building (i.e., global) fragility models as functions of hurricane hazard parameters, building attributes, and their interactions.

1.3 Scope of the Study

This study focuses on fragility modeling of wood-framed single family homes subjected to simultaneous hurricane hazards (i.e., wind, wave, and surge hazards). The building damage and inventory dataset used in the development of the fragility model is based on the MCEER field reconnaissance conducted after 2005 Hurricane Katrina in coastal Mississippi. Hazard intensities (i.e. maximum significant wind speed, maximum storm surge height, maximum significant wave height, maximum water speed) were obtained from field-validated Advanced CIRCulation (ADCIRC) and Simulating WAves Nearshore (SWAN) models (Dietrich et al., 2012) run by Dr. J. Casey Dietrich at North Carolina State University. The predictive data-based fragility models estimate damage state (DS) exceedance probabilities and the probability of collaspe, first as a function of hazard parameters and their interactions, and second as a function of hazard parameters, building attributes (i.e., foundation type, number of stories), and the interaction of hazard parameters and building attributes. Due to the large number of destroyed buildings in coastal Mississippi after Hurricane Katrina, almost 45% of data for foundation type and number of stories, described as slab and elevated, and one- and two-story, respectively, were missing; therefore, logistic regression imputation models are used to impute the missing observations. Diagnostic and comparison approaches are developed to evaluate the performance of the logistic regression imputation models.

1.4 Organization of the Dissertation

This dissertation is organized by objective topics: Chapter 2 presents a methodology for developing predictive data-based fragility models for single family homes subjected to combined wind, wave, and flood hazards without consideration of building attributes. Chapter 3 presents imputation techniques and novel diagnostic and comparison approaches for binary categorical variables (i.e., building attributes) with missing observations. Chapter 4 presents a methodology for developing predictive data-based fragility models for single family homes subjected to combined wind, wave, and flood hazards, taking into consideration building attributes that were directly observed or imputed in Chapter 3.

CHAPTER 2. PREDICTIVE DATA-BASED FRAGILITY MODEL FOR SINGLE FAMILY HOMES SUBJECTED TO WIND, WAVE, AND FLOOD HAZARDS

2.1 Introduction

Building vulnerability for multi-hazard (e.g., wind, surge, wave) hurricane events has been considered primarily through the use of analytical models (e.g., Barbato et al., 2013; Choine et al., 2015; Lee & Rosowsky, 2006; Li & Ellingwood, 2009a, 2009b; Li & van de Lindt, 2012; Li et al., 2011; Liu et al., 2015; Schmidt et al., 2011). However, significant modeling challenges remain, including derivation of the joint hazard distribution, consideration of overlapping spatial and temporal hazard effects, validation of developed models, and reflection of the population and variability of the built environment, requiring significant input data and computation capabilities. These issues hinder the development of comprehensive multi-hazard hurricane fragility models. A critical issue in model validation is the lack of observed data (Baradaranshoraka et al., 2017; Ellingwood et al., 2004), which prevents quantification of model prediction accuracy.

Multi-hazard fragility models have been considered infrequently from a statistical perspective, although current efforts are supporting the validation of analytical models and development of robust statistical models. These efforts include the National Institute of Standards and Technology development of Disaster and Failure Studies data repositories (NIST National Institute of Standards and Technology, 2011) after hazard events (e.g., hurricane, tornado, fire) and the Pacific Earthquake Engineering Research Center development of an earthquake ground motion database (PEER Pacific Earthquake Engineering Research Center, 2011). Data-based statistical models represent damage as a function of multiple hazards, use observed data to fit the model and assess its prediction accuracy, and consider variability in building and environmental attributes (Pitilakis et al., 2014). These characteristics are of particular value for non-engineered

or marginally engineered buildings (e.g., single family homes), where building parameters are unavailable or impractical to model for individual buildings.

Fragility models are used to estimate the probability of being in or exceeding a specified damage state or collapse, conditional on one or more hazards. Data-based statistical fragility models are classified as explanatory or predictive models. Explanatory models are developed primarily for inference and interpretation of model coefficients in the same population from which sample data are obtained, where model performance is validated on the same set of buildings used to develop the model. On the other hand, predictive models are developed for use in populations outside that used to obtain sample data. The model's performance is externally validated on a new sample of buildings. Said differently, the training model is applied to test data for external predictive or classification purposes. Unlike explanatory models, predictive models are opportunistically built with the goal of predicting future damage for a new set of buildings in a hazard environment. Assessment of predictive models is measured by the predictive accuracy, often using metrics computed from external cross-validation (Geisser, 1975; Stone, 1974).

Recently, data-based fragility models have been implemented to model multi-hazard hurricane building fragility. Tomiczek et al. (2014a) fitted and compared six multiple linear regression models to estimate the probability of collapse for pile-elevated, wood-framed buildings as a function of combinations of maximum significant wave height, breaking wave height, maximum current velocity, freeboard height, and building age. Freeboard height above wave crests, maximum significant wave height, maximum current velocity, and construction date were found to be the most important variables that contribute significantly to collapse probability. Tomiczek et al. (2017) classified building damage into seven DS and used multiple linear regression to estimate probability of damage as a function of relative shielding, age, maximum

water velocity, maximum water depth, and minimum freeboard. Maximum water velocity and relative shielding were found to be the most important variables that significantly contribute to building damage.

However, in both previous studies, the categorical dependent variables (non-collapse/collapse and the seven DS) were modeled as continuous numerical variables, which may result in probabilities greater than one or less than zero, and can have inefficient standard errors for the estimated coefficients since the discrete nature of the response was not modelled. Additionally, a measurement of relative residual variance to evaluate model fitting was used. While relative residual variance can be useful for comparison across models, it may be of limited use for prediction accuracy due to the discrete nature of the response variable.

Hatzikyriakou et al. (2015) developed a component-based logistic regression fragility model to predict the probability of collapse for single-family home foundations, exterior walls, and siding as a function of environmental and building attributes, namely, distance from the coast, ground elevation, elevation of the lowest horizontal member, structure height above lowest horizontal member, house age, and building perimeter. Distance from the coast, ground elevation, and house age were found to be significant damage predictors for component failure. Although the categorical binary response variable was modeled correctly, the model was limited to inference and interpretation of the model coefficients without any evaluation of model performance.

General deficiencies within current hurricane data-based statistical fragility models are twofold: (1) the crude use of classical modeling approaches for what is truly a binomial or multinomial response, and (2) the limited use of external validation to evaluate model performance. Specifically, while multiple linear regression explains the relationship between damage and explanatory variables, logistic regression and proportional odds cumulative logit

models represent the true nature and distribution of the response variables for binomial and multinomial dependent variables, respectively, while also providing meaningful interpretations in terms of odds ratios. While model fit is paramount, external validity provides a realistic evaluation of model prediction accuracy when applied to field data, for example to predict future damage. In this context, external validation is an improvement over the current multi-hazard data-based statistical fragility models.

2.1.1 Aim

The aim of Chapter 2 is to develop predictive data-based multi-hazard, hurricane fragility models for single-family homes for ordered categorical DS and binary collapse/non-collapse. The models are developed as a function of maximum hurricane hazard variables (i.e., wind speed, significant wave height, surge depth, water speed) at the individual building scale. Videographic damage data recorded in coastal Mississippi after 2005 Hurricane Katrina and simulated hazard data computed by the tightly-coupled Simulating WAves Nearshore and ADvanced CIRCulation (SWAN+ADCIRC) model are used as model inputs. Global building damage (i.e., description of the overall building damage) is assessed using the seven-category Wind and Flood (WF) Damage Scale developed by Friedland and Levitan (2009). The probability of being in or exceeding a specified DS and the probability of collapse are estimated using proportional odds cumulative logit and logistic regression models, respectively. External cross-validation (CV) is performed to evaluate model prediction accuracy, specifically using "leave-one-out" cross-validation (LOOCV) and expressed in terms of the cross-classification rate (CCR).

2.2 Data

2.2.1 Global Building Damage State Response Variable

Hurricane Katrina made landfall on 29 August 2005 as a Saffir-Simpson Category 3 hurricane with 1-minute sustained winds of 56 m/s (124 mph) near Buras, Louisiana, and then as

a Category 3 hurricane with 53 m/s (118 mph) 1-minute sustained winds near the Louisiana-Mississippi border with storm surge depth of 8.5 m (28 feet) at Pass Christian, Mississippi (Fritz et al., 2008). An MCEER rapid reconnaissance was conducted on 6-11 September 2005 using the VIEWS^{TM} system (Adams et al., 2004) to capture georeferenced video of buildings in coastal Mississippi, specifically Hancock, Harrison, and Jackson Counties (Figure 2.1).

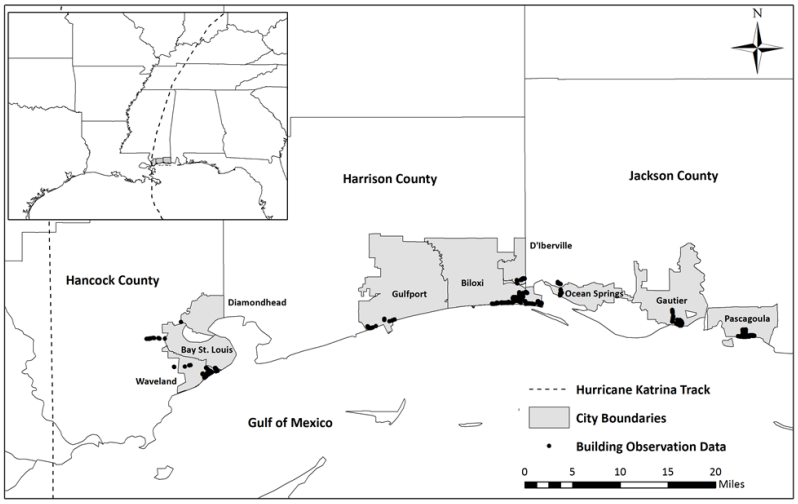

Figure 2.1 Hurricane Katrina track, study areas, and building observation locations

The field data collection consisted of acquisition of geo-referenced high-resolution video captured from the passenger side of a slowly moving vehicle. The goal of the reconnaissance was to document the extent of damage in the near aftermath of the hurricane. No specific sampling strategy was implemented and the collected data reflect limitations of accessibility and data collection time, including impassibility of routes and the presence of debris piles and emergency vehicles obscuring data collection. Therefore, a degree of uncertainty is inherent in the data collection and damage assessment that is not considered in this analysis.

After the reconnaissance was completed, the videos and still images extracted from these videos were reviewed to document building attributes and DS. Every building along the driving route was surveyed by assessing damage to the portions of the buildings captured on the videos

(e.g., front and side of the building). Building roof damage was assessed using post-event National Oceanic and Atmospheric Administration (NOAA) aerial color images with 0.3 m spatial resolution. The global building DS response variable (*Y*) was derived from visual damage assessment of each surveyed building using the Wind and Flood (WF) Damage Scale developed by Friedland and Levitan (2009). The WF Damage Scale categorizes global combined wind and flood residential building damage into seven damage levels, *j*, ranked WF0 through WF6 based on ten criteria. The WF Damage Scale has also been further modified and applied by Tomiczek et al. (2017) Zhang et al. (2017), and Hatzikyriakou (2017) to classify building damage data obtained from field reconnaissance.

The study area was limited to the initial surge inundation extents delineated by the Federal Emergency Management Agency (FEMA). A geographic information systems (GIS) database was developed that includes land parcel data and building footprint polygons. The calculated centroid for each building footprint was used to represent the building location in the study area. Single-family homes were typically wood-framed, one-and two-story homes with brick or siding cladding, and built on slabs or elevated foundations. Few buildings with foundation types and numbers of stories differing from these predominant characteristics were found in the study area. Such buildings, along with those having unassessed DS, were excluded from the analysis, resulting in a final dataset describing the global building DS for 866 single- family homes (Table 2.1).

Table 2.1 Global building damage states and frequency of collected data

Levels, *j*	Damage states	Number of buildings	Percent of buildings
1	WF0=No damage	4	0.46%
2	WF1=Minor damage	7	0.81%
3	WF2=Moderate damage	60	6.96%
4	WF3=Severe damage	349	40.30%
5	WF4=Very severe damage	45	5.20%
6	WF5=Partial collapse	42	4.85%
7	WF6=Collapse	359	41.45%

For categorical variables, it is generally recommended that a minimum of 50 samples be collected for each variable level (Lillesand et al., 2014). However, low sample numbers in WF0, WF1, WF4, and WF5 indicate that issues in model fitting may be encountered. Therefore, WFDS were aggregated to represent the global building DS response variable *Y* for *n* models, each with *j* levels, $DS_{j,n}$ (Table 2.2). Models 1 through 37 have ordered multinomial response variables, while Models 38 and 39 have a binary response variable.

Table 2.2 Model (*n*), number of observations in each *WFDS*, and global building DS response variable levels for each model, $DS_{j,n}$.

Model (*n*)	WF0	WF1	WF2	WF3	WF4	WF5	WF6
No. Obs.	4	7	60	349	45	42	359
1	$DS_{1,1}$	$DS_{2,1}$	$DS_{3,1}$	$DS_{4,1}$	$DS_{5,1}$	$DS_{6,1}$	$DS_{7,1}$
2	$DS_{1,2}$			$DS_{2,2}$	$DS_{3,2}$	$DS_{4,2}$	$DS_{5,2}$
3	$DS_{1,3}$			$DS_{2,3}$	$DS_{3,3}$	$DS_{4,3}$	
4	$DS_{1,4}$			$DS_{2,4}$		$DS_{3,4}$	
5	$DS_{1,5}$			$DS_{2,5}$		$DS_{3,5}$	$DS_{4,5}$
6	$DS_{1,6}$			$DS_{2,6}$	$DS_{3,6}$		
7	$DS_{1,7}$			$DS_{2,7}$			$DS_{3,7}$
8	$DS_{1,8}$				$DS_{2,8}$	$DS_{3,8}$	$DS_{4,8}$
9	$DS_{1,9}$				$DS_{2,9}$		$DS_{3,9}$
10	$DS_{1,10}$				$DS_{2,10}$	$DS_{3,10}$	
11	$DS_{1,11}$		$DS_{2,11}$	$DS_{3,11}$	$DS_{4,11}$	$DS_{5,11}$	$DS_{6,11}$
12	$DS_{1,12}$		$DS_{2,12}$		$DS_{3,12}$	$DS_{4,12}$	$DS_{5,12}$
13	$DS_{1,13}$		$DS_{2,13}$			$DS_{3,13}$	$DS_{4,13}$
14	$DS_{1,14}$		$DS_{2,14}$				$DS_{,314}$
15	$DS_{1,15}$		$DS_{2,15}$		$DS_{3,15}$		$DS_{4,15}$
16	$DS_{1,16}$		$DS_{2,16}$			$DS_{3,16}$	
17	$DS_{1,17}$		$DS_{2,17}$		$DS_{3,17}$		
18	$DS_{1,18}$		$DS_{2,18}$	$DS_{3,18}$		$DS_{4,18}$	
19	$DS_{1,19}$		$DS_{2,19}$	$DS_{3,19}$			$DS_{4,19}$
20	$DS_{1,20}$		$DS_{2,20}$	$DS_{3,20}$	$DS_{4,20}$		
21	$DS_{1,21}$		$DS_{2,21}$	$DS_{3,21}$	$DS_{4,21}$		$DS_{5,21}$
22	$DS_{1,22}$		$DS_{2,22}$	$DS_{3,22}$		$DS_{4,22}$	$DS_{5,22}$
23	$DS_{1,23}$		$DS_{2,23}$	$DS_{3,23}$	$DS_{4,23}$	$DS_{5,23}$	
24	$DS_{1,24}$	$DS_{2,24}$		$DS_{3,24}$	$DS_{4,24}$	$DS_{5,24}$	$DS_{6,24}$
25	$DS_{1,25}$	$DS_{2,25}$			$DS_{3,25}$	$DS_{4,25}$	$DS_{5,25}$
26	$DS_{1,26}$	$DS_{2,26}$				$DS_{3,26}$	$DS_{4,26}$
27	$DS_{1,27}$	$DS_{2,27}$					$DS_{3,27}$
28	$DS_{1,28}$	$DS_{2,28}$		$DS_{3,28}$		$DS_{4,28}$	
29	$DS_{1,29}$	$DS_{2,29}$		$DS_{3,29}$			$DS_{4,29}$
30	$DS_{1,30}$	$DS_{2,30}$		$DS_{3,30}$			
31	$DS_{1,31}$	$DS_{2,31}$		$DS_{3,31}$	$DS_{4,31}$		$DS_{5,31}$
32	$DS_{1,32}$	$DS_{2,32}$		$DS_{3,32}$	$DS_{4,32}$		
33	$DS_{1,33}$	$DS_{2,33}$		$DS_{3,33}$	$DS_{4,33}$	$DS_{5,33}$	

Table 2.2 Continued

Model (n)	WF0	WF1	WF2	WF3	WF4	WF5	WF6
34	$DS_{1,34}$	$DS_{2,34}$	$DS_{3,34}$		$DS_{4,34}$	$DS_{5,34}$	$DS_{6,34}$
35	$DS_{1,35}$	$DS_{2,35}$	$DS_{3,35}$			$DS_{4,35}$	$DS_{5,35}$
36	$DS_{1,36}$	$DS_{2,36}$	$DS_{3,36}$				$DS_{4,36}$
37	$DS_{1,37}$	$DS_{2,37}$	$DS_{3,37}$				
38	$DS_{1,38}$						$DS_{2,38}$
39	$DS_{1,39}$					$DS_{2,39}$	

2.2.2 Computationally-Modeled Explanatory Hazard Variables

Simulation of maximum wind speed, maximum water level, maximum significant wave height, and maximum water velocity has been characterized using the coupled SWAN+ ADCIRC models. The modeling was performed by Dr. Casey Dietrich from North Carolina State University, with the methodology provided in Appendix A.

While 10-minute sustained wind speeds were used as forcing in the wave and surge models, an averaging time of 3-seconds is more appropriate to explain building damage (American Society of Civil Engineers (ASCE), 2010). Maximum 10-minute wind speeds at each building location $\left(U_{10,max}\right)$ were converted to maximum 3-second gust wind speeds $\left(U_{3,max}\right)$. The Durst gust factor curve (Durst, 1960) is commonly used to convert between wind speed averaging times; however, Krayer and Marshall (1992) found that the gust factors associated with hurricane winds were higher than those associated with wind speeds from extratropical cyclones obtained from the Durst curve. The Krayer-Marshall gust factor model has been used widely for converting between averaging times of hurricane wind speeds (e.g., Powell & Houston, 1996; Vickery & Twisdale, 1995; Vickery et al., 2000). The appropriate U_t/U_{3600} gust factors for t = 3 seconds and t = 10 minutes (600 seconds) were obtained from the Krayer-Marshall gust curve and the maximum 3-second gust wind speed was determined at each building location in the study area.

Table 2.3 lists the quantitative explanatory variables (X_h) used to fit the fragility models, which are the maximum values of the time series obtained from the coupled SWAN+ADCIRC models. The maximum surge depth (D_{max}) at the centroid of each building footprint was calculated

as the difference between maximum water level (ζ_{max}) and the bathymetry / topography (m) of the SL16 mesh (NAVD88) at that location.

Table 2.3 Explanatory variables used to construct the fragility models.

X_h	Symbol	Description	Range
x_1	$U_{3,\max}$	Maximum 3-second gust wind speed	[47.63-67.99] m/s
x_2	$H_{S,max}$	Maximum significant wave height	[0-3.20] m
x_3	D_{max}	Maximum surge depth above local ground	[0-7.94] m
x_4	U_{max}	Maximum water speed	[0-2.80] m/s

2.2.3 Multicollinearity

Multicollinearity among independent variables is evaluated using the variance inflation factor *(VIF*). The *VIF* for X_h is given as $VIF_h = \frac{1}{1-R_h^2}$, where R_h^2 is the coefficient of determination for a multiple regression model, considering X_h is the dependent variable and the remaining explanatory variables are independent variables. A value for VIF_h greater than 10 indicates that X_h is almost a perfect linear combination of other explanatory variables. The multicollinearity among quantitative explanatory variables (X_h) was tested and positive correlation was found for maximum significant wave height and maximum surge depth. The coefficient of determination for the maximum significant wave height regression model was found to be $R^2_{H_{S,max}}$ = 0.968, resulting in $VIF_{H_{S,max}}$ = 15.88. The coefficient of determination for the maximum surge depth regression model was found to be $R^2_{D_{max}}$ = 0.963, resulting in $VIF_{D_{max}}$ = 13.99. No correlation was found between both maximum 3-second gust wind speed and maximum water speed with any of the other hazard variables with $VIF_{U_{3,\max}}$ = 2.53 and $VIF_{U_{max}}$= 2.21. With multicollinearity, one predictor variable may have reversed effect on the response variable because it overlaps with other predictors in the model. Additionally, multicollinearity may lead to both variables being insignificant when

included in the same model and will inflate the standard errors of the model coefficients. With this said, $H_{\mathrm{S,max}}$ and D_{max} are not included in the same fragility model.

2.3 Fragility Modeling

Binary logistic regression models, also called logit models, evaluate one dichotomy (e.g., success or failure). The generalized form of the binary logistic regression model is given as

$$\mathrm{logit}[P] = \ln\left[\frac{P}{1-P}\right] = \alpha + \sum_{h=1}^{H} \beta_h x_h \,, \tag{2.1}$$

where P denotes the probability of "success," which is defined in this study as collapse; $\mathrm{logit}[P]$ is the logit link function, which is equal to the natural logarithm (log) of the odds of collapse; α is the model intercept; and β_h are model coefficients. The odds of collapse are defined as the ratio of the probability of success to its complement. Logistic regression models have been used previously to model hurricane building component damage (Hatzikyriakou et al., 2015), tsunami building damage (Reese et al., 2011), and hurricane power system damage (Reed et al., 2016).

Extending binary logistic regression models, the dependence of an ordered categorical multinomial response (e.g., DS) on discrete or continuous covariates is modeled as a series of dichotomies using the proportional odds cumulative logit model, which uses cumulative probabilities to evaluate ordered categories with the assumption that curves of the various cumulative logits are parallel (i.e., proportional odds assumption). Proportional odds cumulative logit models also have been used previously to model tsunami building damage (Charvet et al., 2014a; Charvet et al., 2014b; Charvet et al., 2015) and earthquake building damage (Lallemant et al., 2015).

For response variable Y with ordinal levels 1 to J (Table 2.2) and H explanatory variables $x_1, x_2, \ldots, x_H$ (Table 2.3), the log odds of response Y in level j or greater is calculated for $j \geq 2$ as

$$logit[P(Y \geq j)] = \ln\left[\frac{P(Y \geq j)}{1-P(Y \geq j)}\right] = \alpha_j + \sum_{h=1}^{H} \beta_h x_h \quad \text{for } j=2\ldots J. \tag{2.2}$$

The odds of the response variable *Y* being in level *j* or greater are defined as the ratio of the probability of *Y* being in level *j* or greater $P(Y \geq j)$ to its complement. The log odds of *Y* being in level *j*=1 or greater is undefined; therefore Equation 2.2 results in a set of $J - 1$ equations with unique intercepts (α_j) and a common slope (β_h) for each of the *H* explanatory variables.

To interpret the influence of increasing hazard intensities on damage, the hazard-specific odds ratio (OR_h) for two values of x_h (i.e., x_{h1}, x_{h2}) with unit increase (i.e., where $x_{h2} - x_{h1} = 1$) is calculated as

$$\mathrm{OR}_{h(1,2)} = \exp[\beta_h(x_{h2} - x_{h1})] = \frac{P(Y \geq j|X_h=x_{h1})/P(Y<j|X_h=x_{h1})}{P(Y \geq j|X_h=x_{h2})/P(Y<j|X_h=x_{h2})}, \tag{2.3}$$

Given that the hazard data (x_h) are continuous variables, OR_h describes numerically the odds of a building being in a higher damage level rather than a lower damage level for each unit increase in x_h, holding all other variables constant. However, a one-unit increase in hazard intensity may not provide the most meaningful representation for OR_h, depending on the hazard. Multiple or fraction of unit increase rather than one unit increase of hazard intensities may provide a better context. For practical interpretation of MOR_h, researchers can choose a scaling factor, M_h, to represent the effect of increasing hazard intensity on the odds ratio. We see where Equation 2.3 is modified to represent an *M* unit increase in hazard intensity. The modified odds ratio (MOR_h) for two values of x_h (i.e.,x_{h1}, x_{h2}) with *M* unit increase (i.e., where $x_{h2} - x_{h1} = M$) is calculated using factored model coefficients ($M_h\beta_h$). An estimate of MOR_h is given as $\exp\left(M_h * \hat{\beta}_h\right)$, while 95% lower (LCI) and upper (UCI) confidence intervals ($\mathrm{MOR}_h\mathrm{CI}_{95\%}$) of the MOR_h is given as $\exp\left[M_h\left(\hat{\beta}_h \pm 1.96 * \mathrm{SE}\left(\hat{\beta}_h\right)\right)\right]$. Where $\hat{\beta}_h$ are the estimated model coefficients, and $\mathrm{SE}\left(\hat{\beta}_h\right)$ is the standard error of the estimated model coefficients $\hat{\beta}_h$.

To reflect the effect of one hazard intensity on damage based on the value of another hazard intensity, the interaction between hazards is represented as the sum of hazard product terms "$x_h x_q$."The log odds of response Y in level *j* or greater is calculated for $j \geq 2$ as

$$logit[P(Y \geq j)] = \ln\left[\frac{P(Y \geq j)}{1-P(Y \geq j)}\right] = \alpha_j + \sum_{h=1}^{H} \beta_h x_h + \sum_{1 \leq h < q \leq H}^{\mathrm{H}} \beta_{hq} x_h x_q \text{ for } j=2\ldots J. \quad (2.4)$$

where β_{hq} are the coefficients associated with any two hazards. Variables x_h and x_q are two hazard terms where $q > h$. All model coefficients are estimated using Maximum Likelihood Estimation (MLE).

The estimated probability of *Y* being in or exceeding level *j* is calculated for $j \geq 2$ as

$$P(Y \geq j) = \frac{\exp\left(\alpha_j + \sum_{h=1}^{H} \beta_h x_h + \sum_{1 \leq h < q \leq H}^{\mathrm{H}} \beta_{hq} x_h x_q\right)}{1+\exp\left(\alpha_j + \sum_{h=1}^{H} \beta_h x_h + \sum_{1 \leq h < q \leq H}^{\mathrm{H}} \beta_{hq} x_h x_q\right)} \quad \text{for } j=2\ldots J. \quad (2.5)$$

The estimated probability of *Y* being in or exceeding the first level (j=1) is equal to one. Solving for $P(Y = j)$, the estimated probability that the DS falls into a specific level, is calculated for levels $j \leq J-1$ as

$$P(Y = j) = P(Y \geq j) - P(Y \geq j+1) \quad \text{for } j \leq J-1. \quad (2.6)$$

The estimated probability that the DS falls into level *J* is equal to the probability of being in or exceeding level *J*, as calculated in Equation 2.5. With interaction terms, interpretation of the odds ratios becomes more involved since the influence of increasing hazard intensities on damage now depends on levels of other hazards.

2.4 Model Fitting and Evaluation

SAS software (Version 9.4) is used to fit the fragility model. For each Model (*n*), two models with three hazard variables are fitted based on Equation 2.2, resulting in a total of 78 models. These models are described with (x_1, x_2, and x_4), and (x_1, x_3, and x_4) hazard variables. Four criteria are used to evaluate the fit and prediction of the 78 models. The first two are of the form

of rejection criteria for screening purposes, while the last two are qualitative criteria used to further narrow the net of the non-rejected models.

1. Satisfaction of model requirements (proportional odds assumption and goodness of fit). For proportional odds cumulative models, the proportional odds assumption assumes that the coefficients for each hazard predictor must be equal across all DS levels and is tested using the chi-square test. For the logistic regression model, the Hosmer and Lemeshow test is used to assess goodness of fit based on the chi-square test. The data are grouped based on a partitioning of the estimated probabilities, then the test compares the observed and fitted counts of the groups. Any model with chi-square p-value < 0.05 is rejected.
2. Statistical significance of model parameters. At least one main hazard effect must be significant or the model is rejected.
3. Reasonableness of response variable model. Once models that pass the rejection criteria are identified, this subjective parameter is used to evaluate the most reasonable model(s) for prediction. Models with high prediction accuracy but with unreasonable response variable grouping (e.g., minor damage falls into the same level as severe damage) are considered less reasonable models for damage prediction.
4. Balance between CCR and class error. Once models that pass the rejection criteria are identified, this criterion is used to evaluate the most reasonable model(s) for prediction. Models with high prediction accuracy (i.e., high value of CCR) but with high class error are considered less reasonable models for damage prediction.

Among the 78 models, models satisfying Criterion 1 are evaluated for Criterion 2. Models satisfying the two rejection criteria are then refitted based on Equation 2.3 to include hazard interaction terms and are re-evaluated based on the two rejection criteria. Models with interaction

terms are described as 1) one model with three main hazard variables and three hazard interaction terms, 2) three models with three main hazard variables and two hazard interaction terms, and 3) three models with three main hazard variables and one hazard interaction term.

2.5 Model Validation

Prediction accuracy for logistic regression and proportional odds cumulative logit models is often evaluated using external cross-validation. When external test data are not available, *k*-fold cross-validation is one of the most widely used approaches to assess external prediction. In *k*-fold cross-validation, the data are partitioned into *k* subsamples, with *k*–1 subsamples used for fitting the model, while the remaining one is used for model validation. The process is cycled through all partitions, each in turn predicting the left out partition using the model that has been trained on all other partitions. Due to sample size considerations, our research implements a special case of *k*-fold cross-validation, namely leave-one-out cross-validation (LOOCV), where *k* is equal to the number of observations (*N*) in the dataset. Models that satisfied the rejection criteria are fitted *N* times, with one observation left out at each fit. For each fit, the predicted DS $\left(\widehat{DS}\right)$ for every left out observation is estimated as follows:

- For the proportional odds cumulative logit models, the estimated probabilities that a DS falls into specific level *j* is calculated based on Equation 2.6, and then the DS corresponding to the highest estimated probability is assigned as the predicted DS $\left(\widehat{DS}\right)$. The process is repeated for every left out observation.
- For the logistic regression model, the estimated probability of collapse is calculated as $P = \frac{\exp\left(\alpha+\sum_{h=1}^{H}\beta_h x_h\right)}{1+\exp\left(\alpha+\sum_{h=1}^{H}\beta_h x_h\right)}$. If the estimated probability of collapse is greater than 0.5, collapse is assigned, otherwise no collapse is assigned. The process is repeated for every left out observation.

For every satisfactory model and after assigning the predicted DS $(\widehat{DS})$ for every left out observation, an error matrix with *N* total observations is constructed. Rows (*d*) of the matrix represent the frequency (z) of observed DS, while columns (*c*) represent the frequency of predicted DS $(\widehat{DS})$, summed across the *N* left out observations of the model. The percentage of correctly classified damage states, expressed as the cross-classification rate (CCR; Equation 2.7), is calculated as

$$CCR = \frac{\sum_{c=1}^{C} z_{cc}}{\sum_{c=1}^{C}\sum_{d=1}^{D} z_{cd}}, \tag{2.7}$$

where z_{cc} are observations along the diagonal of the error matrix, and z_{cd} are all observations in the error matrix. The percentage of misclassified DS for each *d*, expressed as class error (CE), is calculated as $CE_d = 1 - \frac{z_{cc}}{\sum_{c=1}^{C} z_{cd}}$.

2.6 Results and Discussion

2.6.1 Fragility Fitting

Based on Equations 2.1 and 2.2, Models 8, 9, 10, 25, 26, and 27 with hazard variables $U_{3,\max}$, $H_{s,max}$, and U_{max}, and Model 38 with hazard variables $U_{3,\max}$, D_{max}, and U_{max} satisfied the two rejection criteria, while the remainder of the models failed to meet the first rejection criterion and were not further tested for Criterion 2. When hazard interaction terms were included (Equation 2.3), no interaction terms were found to be significant. Therefore, none of the models with hazard interaction terms satisfied the two rejection criteria and these models were therefore removed from further consideration. Table 2.4 contains the estimated coefficients, standard error, *p*-value, factored model coefficients, MOR_h, and LCI and UCI of $MOR_hCI_{95\%}$ for models that met the rejection criteria. Factored model coefficients, MOR_h, and $MOR_hCI_{95\%}$ were calculated using

$M_{U_{3,\max}} = 4.5$ (m/s), $M_{H_{S,\max}} = 0.3$ (m), $M_{D_{max}} = 1$ (m), and $M_{U_{max}} = 0.5$ (m/s). Asterisks appearing after *p*-values denote statistically significant parameters at the 5% level.

Table 2.4 Parameter estimates, standard error, *p*-value, MOR_h and $MOR_hCI_{95\%}$ for models satisfying rejection criteria with no significant interaction terms

								$MOR_hCI_{95\%}$	
Model	Coefficient	Parameter	Estimated	Std. Error	*p*-value	$M_h\beta_h$	MOR_h	LCI	UCI
8	$\hat{\alpha}_2$	Intercept 2	-7.66	1.55	<0.0001*	-	-	-	-
	$\hat{\alpha}_3$	Intercept 3	-8.08	1.55	<0.0001*	-	-	-	-
	$\hat{\alpha}_4$	Intercept 4	-8.5	1.55	<0.0001*	-	-	-	-
	$\hat{\beta}_1$	$U_{3,\max}$	0.05	0.03	0.0722	0.23	1.26	0.96	1.63
	$\hat{\beta}_2$	$H_{S,\max}$	4.13	0.32	<0.0001*	1.24	3.46	2.86	4.17
	$\hat{\beta}_3$	U_{max}	1.11	0.66	0.0938	0.56	1.75	0.91	3.33
9	$\hat{\alpha}_2$	Intercept 2	-7.63	1.55	<0.0001*	-	-	-	-
	$\hat{\alpha}_3$	Intercept 3	-8.47	1.55	<0.0001*	-	-	-	-
	$\hat{\beta}_1$	$U_{3,\max}$	0.05	0.03	0.0750	0.23	1.26	0.96	1.63
	$\hat{\beta}_2$	$H_{S,\max}$	4.12	0.32	<0.0001*	1.24	3.46	2.85	4.15
	$\hat{\beta}_3$	U_{max}	1.16	0.67	0.0829	0.58	1.79	0.93	3.44
10	$\hat{\alpha}_2$	Intercept 2	-7.77	1.59	<0.0001*	-	-	-	-
	$\hat{\alpha}_3$	Intercept 3	-8.19	1.59	<0.0001*	-	-	-	-
	$\hat{\beta}_1$	$U_{3,\max}$	0.05	0.03	0.0665	0.23	1.26	0.96	1.63
	$\hat{\beta}_2$	$H_{S,\max}$	4.02	0.33	<0.0001*	1.21	3.35	2.75	4.06
	$\hat{\beta}_3$	U_{max}	1.43	0.74	0.0522	0.72	2.05	0.99	4.22
25	$\hat{\alpha}_2$	Intercept 2	0.28	1.45	0.8494	-	-	-	-
	$\hat{\alpha}_3$	Intercept 3	-7.45	1.5	<0.0001*	-	-	-	-
	$\hat{\alpha}_4$	Intercept 4	-7.9	1.5	<0.0001*	-	-	-	-
	$\hat{\alpha}_5$	Intercept 5	-8.3	1.5	<0.0001*	-	-	-	-
	$\hat{\beta}_1$	$U_{3,\max}$	0.04	0.03	0.1016	0.18	1.2	0.92	1.56
	$\hat{\beta}_2$	$H_{S,\max}$	4.22	0.32	<0.0001*	1.27	3.56	2.94	4.28
	$\hat{\beta}_3$	U_{max}	1.24	0.67	0.0660	0.62	1.86	0.96	3.58
26	$\hat{\alpha}_2$	Intercept 2	0.06	1.56	0.9674	-	-	-	-
	$\hat{\alpha}_3$	Intercept 3	-8.39	1.66	<0.0001*	-	-	-	-
	$\hat{\alpha}_4$	Intercept 4	-8.82	1.66	<0.0001*	-	-	-	-
	$\hat{\beta}_1$	$U_{3,\max}$	0.05	0.03	0.0875	0.23	1.26	0.96	1.63
	$\hat{\beta}_2$	$H_{S,\max}$	4.39	0.35	<0.0001*	1.32	3.74	3.04	4.59
	$\hat{\beta}_3$	U_{max}	0.93	0.69	0.1797	0.47	1.6	0.81	3.13
27	$\hat{\alpha}_2$	Intercept 2	-0.12	1.75	0.9470	-	-	-	-
	$\hat{\alpha}_3$	Intercept 3	-9	1.85	<0.0001*	-	-	-	-
	$\hat{\beta}_1$	$U_{3,\max}$	0.05	0.03	0.1185	0.23	1.26	0.96	1.63
	$\hat{\beta}_2$	$H_{S,\max}$	4.5	0.38	<0.0001*	1.35	3.86	3.09	4.59
	$\hat{\beta}_3$	U_{max}	0.89	0.72	0.2178	0.45	1.57	0.81	3.13
38	$\hat{\alpha}$	Intercept	-18.00	1.92	<0.0001*	-	-	-	-
	$\hat{\beta}_1$	$U_{3,\max}$	0.22	0.03	<0.0001*	0.99	2.69	2.07	3.51
	$\hat{\beta}_2$	D_{max}	0.99	0.10	<0.0001*	0.99	2.69	1.27	1.43
	$\hat{\beta}_3$	U_{max}	2.32	0.69	0.0008*	1.16	3.19	1.62	6.27

* Significant at α= 0.05

For all DS models, the only statistically significant hazard variable was the maximum significant wave height, while maximum 3-second gust wind speed and maximum water speed were not found to significantly affect damage. The results show that the primary DS determinant for buildings subjected to wind, wave, and water speed is the maximum significant wave height. However, the *p*-value (0.0522) of the maximum water speed coefficient ($\hat{\beta}_3$) is on the border of the significance level (α= 0.05) for Model 10 and very close to the border of the significance level for Models 8, 9, and 25, which indicates that maximum water speed may have an effect on increasing damage. Kennedy et al. (2010), Tomiczek et al. (2014a), and Tomiczek et al. (2017) also found that significant wave height significantly contributes to damage and should be considered in the development of fragility models. The average odds for maximum significant wave height of the six DS models is 3.57. This is interpreted as: for every 0.3 m (0.98 ft) increase in maximum significant wave height, the odds of being in a higher DS are 3.57 times greater (257% increase in odds), holding all other variables constant. Among all DS models, the odds for maximum water speed were the highest for Model 10, which is interpreted as: for every 0.5 m/s (1.64 ft/s) increase in maximum water speed, the odds of being in a higher DS are 2.05 times greater (105% increase in odds).

For Model 38, which predicts binary collapse/non-collapse, all three hazard variables were statistically significant. The results show that the collapse potential of buildings subjected to wind, surge, and water speed is significantly affected by all three hazards. As any of the hazard variables increase, the odds of collapse increase. Tomiczek et al. (2014a) and Tomiczek et al. (2017) also found that water speed contributes significantly to collapse and damage and should be considered in the development of fragility models. However, these authors excluded wind speed from their analyses without statistical testing. Their assumption was based on the fact that Hurricanes Ike

(2009) and Sandy (2012) had wind speeds lower than common damage initiation thresholds. Similar to Hurricanes Ike and Sandy, Hurricane Katrina was an event with lower wind speeds; however, the maximum 3-second gust wind speed was found to be a significant contributor to collapse. Interpretation of the odds shows that, holding all other variables constant:

- for every 4.5 m/s (10.07 mph) increase in maximum 3-second gust wind speed, the odds of collapse are 2.69 times greater (169% increase in odds)
- for every 0.5 m/s (1.64 ft/s) increase in maximum water speed, the odds of collapse are 3.19 times greater (219% increase)
- for every 1 m (3.28 ft) increase in maximum surge depth, the odds of collapse are 2.69 times greater (169% increase in odds)

2.6.2 Model Validation and Evaluation

LOOCV error matrices for the seven models that satisfied the rejection criteria are provided in Table 2.5. Rows of the tables represent the frequency of observed DS, while columns represent the frequency of predicted DS $(\widehat{DS})$. The *n* subscript in the predicted DS $(\widehat{DS}_n)$ represents the corresponding model number.

Table 2.5 Observed vs. predicted model error matrices, CE, and CCR for non-rejected models

$DS_{j,n}$	$\widehat{DS}_{1,n}$	$\widehat{DS}_{2,n}$	$\widehat{DS}_{3,n}$	$\widehat{DS}_{4,n}$	$\widehat{DS}_{5,n}$	Observed Sum	CE	CCR
$DS_{1,8}$	375	16	7	22	--	420	11%	81%
$DS_{2,8}$	21	5	1	18	--	45	89%	
$DS_{3,8}$	18	2	1	21	--	42	98%	
$DS_{4,8}$	23	8	8	320	--	359	11%	
$DS_{1,9}$	370	21	29	--	--	420	12%	81%
$DS_{2,9}$	41	13	33	--	--	87	85%	
$DS_{3,9}$	21	18	320	--	--	359	11%	
$DS_{1,10}$	370	17	33	--	--	420	12%	83%
$DS_{2,10}$	20	5	20	--	--	45	89%	
$DS_{3,10}$	42	19	340	--	--	401	15%	
$DS_{1,25}$	0	4	0	0	0	4	100%	81%

Table 2.5 Continued

$DS_{j,n}$	$\widehat{DS}_{1,n}$	$\widehat{DS}_{2,n}$	$\widehat{DS}_{3,n}$	$\widehat{DS}_{4,n}$	$\widehat{DS}_{5,n}$	Observed Sum	CE	CCR
$DS_{2,25}$	1	380	5	7	23	416	9%	
$DS_{3,25}$	0	22	3	1	19	45	93%	
$DS_{4,25}$	0	19	3	1	19	42	98%	
$DS_{5,25}$	1	27	7	4	320	359	11%	
$DS_{1,26}$	1	3	0	0	--	4	75%	
$DS_{2,26}$	1	420	6	34	--	461	9%	85%
$DS_{3,26}$	0	21	2	19	--	42	95%	
$DS_{4,26}$	1	38	3	317	--	359	12%	
$DS_{1,27}$	1	3	0	--	--	4	75%	
$DS_{2,27}$	1	440	57	--	--	498	12%	85%
$DS_{3,27}$	1	65	298	--	--	364	18%	
$DS_{1,38}$	450	57	--	--	--	507	11%	87%
$DS_{2,38}$	58	301	--	--	--	359	16%	

Note: -- indicates error terms are not applicable due to the number of damage levels *j* for model *n*.

The results show that the overall model prediction accuracies are high, with CCR ranging from 81% to 87%, although individual DS or several DS have high CE (>50%). High CE were found for all DS levels with few observations.

2.6.3 DS Fragility Models

Model 8 has reasonable grouping of DS; however, the model has two DS with high CE. Models 25 and 26 have three and two DS with high CE, respectively, as well as unreasonable groupings of DS, where $DS_{2,25}$ ranges from minor damage to severe damage and $DS_{2,26}$ ranges from minor damage to very severe damage. Model 27 has the highest prediction accuracy (85%); however, $DS_{2,27}$ has an unreasonable grouping, ranging from minor damage to partial collapse and $DS_{1,27}$ has a high CE (75%). Because of the number of DS with high CE and unreasonable groupings of DS, Models 8, 25, 26, and 27 are excluded from consideration, while Models 9 and 10 are evaluated further. Model 10 has 2% higher prediction accuracy and 4% higher CE than Model 9. However, Model 10 has a more reasonable response variable grouping than Model 9, where $DS_{3,10}$ represents partial collapse and collapse, while $DS_{2,9}$ represents very severe damage and partial collapse. Additionally, the *p*-value (0.0522) for the maximum water speed coefficient

($\hat{\beta}_3$) in Model 10 is on the border of the significance level (α= 0.05). Therefore, Model 10 is chosen as the more reasonable predictive fragility model to predict the probability of being in or exceeding $DS_{2,10}$ and $DS_{3,10}$ as a function of maximum 3-second gust wind speed, maximum significant wave height, and maximum water speed. There is not one specific rule that can be used to select a "final" model between Model 9 and Model 10. Since both models satisfy the rejection criteria, the choice of the model is subjective. Both models are reasonable to be used as a predictive fragility model.

The estimated probability of being in or exceeding $DS_{2,10}$ and $DS_{3,10}$, respectively, as a function of maximum 3-second gust wind speed, maximum significant wave height, and maximum water speed is estimated as

$$logit\left[P(Y \geq \mathrm{DS}_{2,10})\right] = -7.77 + 0.05 * U_{3,\max} + 4.02 * H_{\mathrm{S},\max} + 1.43 * U_{max}, \text{ and} \quad (2.8)$$

$$logit\left[P(Y \geq \mathrm{DS}_{3,10})\right] = -8.19 + 0.05 * U_{3,\max} + 4.02 * H_{\mathrm{S},\max} + 1.43 * U_{max}, \quad (2.9)$$

Figures 2.2 a) and b) show fragility surfaces for Model 10 as a function of maximum significant wave height and maximum water speed considering maximum 3-second wind speed of 62 m/s.

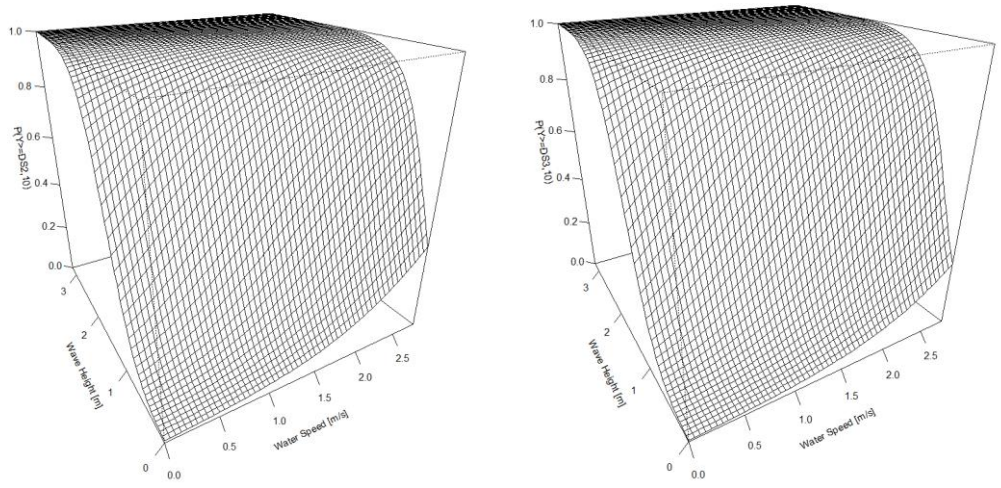

a) b)

Figure 2.2 Probability of being in or exceeding a) $DS_{2,10}$ and b) $DS_{3,10}$ as a function of maximum significant wave height and maximum water speed.

2.6.4 Collapse Fragility Model

Model 38 predicts probability of collapse as a function of maximum 3-second gust wind speed, maximum surge depth, and maximum water speed with 87% prediction accuracy. No high CE values are shown due to large sample sizes. The estimated probability of collapse ($Y \geq \mathrm{DS}_{38,2}$) as a function of maximum 3-second gust wind speed, maximum surge depth, and maximum water speed is given as

$$logit\left[P(Y \geq \mathrm{DS}_{38,2})\right] = -18 + 0.22 * U_{3,\max} + 0.99 * D_{\max} + 2.32 * U_{max} \quad (2.10)$$

Figure 2.3 shows the fragility surface for Model 38 as a function of maximum surge depth and maximum water speed considering maximum 3-second wind speed of 62 m/s.

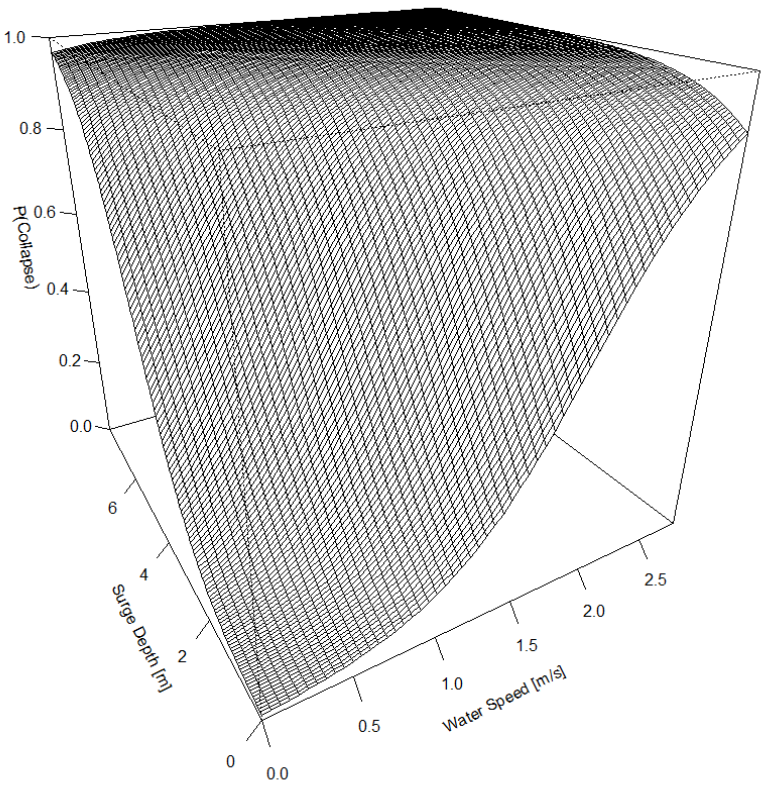

Figure 2.3 Probability of collapse as a function of maximum significant surge depth and maximum water speed.

2.7 Summary and Conclusions

Physical damage to residential buildings from hurricane wind, wave, and storm surge hazards was statistically modeled and hazard attributes that contribute significantly to damage and collapse were determined. Predictive data-based multi-hazard, hurricane fragility models for ordered categorical DS and binary collapse/non-collapse were developed as a function of maximum 3-second gust wind speed, maximum significant wave height, maximum surge depth, and maximum water speed. The proportional odds cumulative logit and logistic regression models were used to estimate the probability of being in or exceeding ordered categorical DS and the probability of collapse, respectively. The findings of this chapter are:

- The proportional odds cumulative logit model showed high accuracy in estimating the probability of being in or exceeding categorical ordered DS as a function of simultaneous hurricane hazards.
- The logistic regression model showed high accuracy in estimating the probability of collapse as a function of simultaneous hurricane hazards.
- Maximum significant wave height was found to be the only significant predictor of damage for DS models, while maximum 3-second gust wind speed, maximum surge depth, and maximum water speed were found to be significant predictors for collapse.
- Maximum water speed was found to be on the border of the significance level for one DS model and very close to the significance level for three DS models.
- High collinearity was found between maximum surge depth and maximum significant wave height, resulting in *VIF* greater than 10. Therefore, models were constructed without the consideration of $H_{\mathrm{S,max}}$ and D_{max} in the same fragility model.

- Low sample numbers in WF0, WF1, WF4, and WF5 resulted in high CE for these DS and any response variable groupings of these DS.
- Application of proportional odds cumulative logit and logistic regression models confirm the effectiveness of statistical models for development of multi-hazard hurricane fragility surfaces and identification of hazard variables that significantly contribute to damage and collapse.

CHAPTER 3. DIAGNOSTIC AND COMPARISON APPROACHES FOR LOGISTIC REGRESSION IMPUTATION MODELS

3.1 Introduction

Missing data are common in nearly all areas of research and have a significant effect on conclusions drawn from the data (Ferrari et al., 2011). Although model-based imputation techniques (e.g., multiple imputation, MI; predictive mean matching, PMM) have become established as standard techniques for handling missing data, approaches to evaluate model performance are limited (Schomaker & Heumann, 2014). Evaluation of imputation model performance is essential to ensure validity and accuracy of the imputed data (Bernhardt, 2018; Cabras et al., 2011; Gelman et al., 2005; Nguyen et al., 2017) and to provide an approach for model comparison and selection among various imputation models (Fay, 1996; Meng, 1994). Current approaches evaluate the performance of one or more imputation models. When an individual imputation model is evaluated, model diagnostics are performed numerically or graphically to determine how well the model estimates missing values. When various imputation models are evaluated, model comparison is performed numerically on statistical models fitted on simulated imputed datasets to determine the model(s) that best meet evaluation criteria (e.g., lowest mean square error, comparing the distributions of the response variable). However, deficiencies in diagnostic and comparison approaches remain.

Existing numerical model diagnostic approaches (e.g., Farhan & Fwa, 2014; Stuart et al., 2009; Zhu et al., 2009) assess the imputation *model* itself and are performed through traditional approaches (e.g., linear regression diagnostics, residual analysis); however, these diagnostic techniques are limited to linear regression-based imputation models and hence, continuous variables. Graphical model diagnostic approaches (e.g., Abayomi et al., 2008; Van Buuren, 2012; White et al., 2011) assess the imputed *values* by visually comparing their distributions with the

distributions of the observed values or by using histograms and boxplots. These techniques yield qualitative evaluations that lose interpretability as the percentage of missingness increases.

On the other hand, model comparison approaches evaluate the performance of several imputation models, and hence various imputation techniques, by performing simulation studies. Akande et al. (2017); Collins et al. (2001); and Raghunathan et al. (2001) simulated datasets with multiple missingness percentages generated from a complete dataset, and then imputed the simulated missing values using imputation techniques. The complete and imputed datasets were used as input to fit statistical models (e.g., linear regression model, logistic regression model). Comparison between the fitted statistical models was then performed by proposing a set of evaluation criteria (e.g., least mean square error values, least model coefficient variances). The model that best satisfied the evaluation criteria was considered to be the best model and used as the basis for identifying the "best" imputation technique. Although model comparison approaches were not limited to one missingness percentage, the evaluation criteria were applied to the statistical models fit using the imputed datasets and not to the imputation models themselves.

Deficiencies in current diagnostic and comparison approaches are in the application of the approaches, where the approaches are either applicable to continuous variables with missing observations or to the statistical models fit using imputed datasets rather than to the imputation models. To my knowledge, no numerical diagnostic approach has been developed to evaluate the performance of imputation models for categorical variables (e.g., binary). This becomes a more significant issue when the application of graphical diagnostic approaches is impractical for data with a high percentage of missingness. On the other hand, application of comparison approaches does not maintain the percentage of missingness in the original dataset, and the approach is applied

to statistical models fit based on simulated datasets with various missingness percentages and not on the imputation models themselves.

3.1.1 Aim and Approach

To address these issues, the aim of Chapter 3 is to develop model diagnostic and comparison approaches that are suited to a known missingness percentage and imputation technique for binary categorical explanatory variables with missing observations. The proposed diagnostic approach numerically evaluates the fit of logistic regression-based imputation models using the logistic regression goodness of fit test. The proposed comparison approach numerically evaluates the performance of the imputation models themselves by finding the percentage of correctly imputed observations, expressed in terms of cross-classification rate (CCR). The diagnostic approach is applied on two model-based imputation techniques, defined as predictive mean matching (PMM) and multiple imputation (MI). The binary explanatory variable with missing observations is used as the response variable for the MI and PMM models, while the rest of the explanatory variables in the complete case dataset are used as the explanatory variables. After fitting and diagnosing the imputation models the comparison approach is applied. Observations from the complete datasets of every binary variable are randomly deleted to accomplish a missingness percentage equal to λ. The MI and PMM imputation models are then used to impute the deleted observations. The percentage of correctly classified observations, expressed as cross-classification rate (CCR), is calculated by comparing prior-and post-deletion values. The imputation model balancing a high CCR and low class error (CE) is chosen as the "final" imputation model.

A dataset collected after 2005 Hurricane Katrina in coastal Mississippi is used for application of the methodology. After Hurricane Katrina and due to the large number of destroyed buildings, almost 45% of the field data describing foundation type and number of stories were

missing. The observed continuous variables (i.e., maximum 3-second wind speed, maximum significant wave height, maximum surge depth, maximum water speed, base flood elevation) describing the hazard parameters and environmental variables are used to impute missing foundation type and number of stories data for slab and elevated foundations of one-and two-story homes.

3.2 Missing Data Imputation

For a dataset with sample size *N*, *G* binary (i.e., levels 0 and 1) explanatory variables $(X_1, X_2, \dots, X_G)$ with missing observations, and *F* continuous explanatory variables $(X_1, X_2, \dots, X_F)$, two model-based imputation techniques T= (T_{PMM}, T_{MI}), defined as predictive mean matching (PMM) and multiple imputation (MI), are applied to impute X_g. For each variable $X_g$with missingness, sample sizes for the complete and missing case subdatasets are $N_{g,cc}$ and $N_{g,miss}$ respectively, where $N_g = N = N_{g,cc} + N_{g,miss}$. Variables of these subdatasets are defined as $X_{g,cc}$, $X_{f,cc}$, $X_{g,miss}$, and $X_{f,miss}$, where the subscript "*CC*" denotes observations of fully-observed X_g, while the subscript "*miss*" denotes observations with missing X_g values. The missing mechanism of the dataset is assumed to be missing at random (MAR), meaning that the probability of missing $X_g$values depends only on the observed variables in the dataset. Based on T, a set of two logistic regression-based imputation models $LR_g = (LR_{g,PMM}, LR_{g,MI})$ is fitted on the $N_{g,CC}$ complete cases. The response variable of LR_g is X_g, and the explanatory variables are X_f.

For T_{PMM}, the imputation procedure imputes a missing value by matching its estimated predictive probability to the nearest complete case estimated predictive probability. A logistic regression model $LR_{g,PMM}$ is fitted on the complete cases as

$$ln\left(\frac{P(X_{g,cc}=1)}{1-P(X_{g,cc}=1)}\right) = \alpha_{g0} + \sum_{f=1}^{F} \alpha_{gf}\, X_{f,cc}\,, \tag{3.1}$$

where $P(X_{g,cc} = 1)$ is the probability of $X_{g,cc}$ being in level 1, α_{g0} is the model intercept, and α_{gf} are model coefficients.

The estimated predictive probability that complete case observations $x_{g,cc}$ with explanatory variables $x_{f,cc}$ belong to level 1 is estimated as

$$P(x_{g,cc} = 1) = \frac{\exp\left(\alpha_{g0}+\sum_{f=1}^{F} \alpha_{gf}\, X_{f,cc}\right)}{1+\exp\left(\alpha_{g0}+\sum_{f=1}^{F} \alpha_{gf}\, X_{f,cc}\right)}, \tag{3.2}$$

The estimated predictive probability that missing observations $x_{g,miss}$ with explanatory variable $x_{f,miss}$ belong to level 1 is estimated as

$$P(x_{g,miss} = 1) = \frac{\exp\left(\alpha_{g0}+\sum_{f=1}^{F} \alpha_{gf}\, X_{f,cc}\right)}{1+\exp\left(\alpha_{g0}+\sum_{f=1}^{F} \alpha_{gf}\, X_{f,cc}\right)}, \tag{3.3}$$

The absolute difference $|D_g|$ between $P(x_{g,miss} = 1)$ and every $P(x_{g,cc} = 1)$ is calculated and used to construct a distance matrix **Q** with number of rows representing the number of complete cases and number of columns representing the number of missing cases. For every column in **Q**, $x_{g,miss}$ is set equal to the $x_{g,cc}$ value corresponding to the row with the smallest $|D_g|$ value. For rows with equal $|D_g|$ values, $x_{g,miss}$ is selected as the mode of the corresponding $x_{g,cc}$ values unless the variable levels are equally represented, in which case, $x_{g,miss}$ is selected at random.

The application of T_{MI} is dependent on the missingness pattern — arbitrary or monotone. For the arbitrary missingness pattern, MI using fully conditional specification (FCS) is used, while MI using logistic regression (LR) is used for the monotone missingness pattern. The imputation procedure for T_{MI} generates M_g imputations by performing draws from the predictive posterior distribution(s) of $X_{g,cc}$ conditioned on $X_{f,cc}$. The number of required imputations M_g depends on

the fraction of missing data λ_g (Rubin, 1978) and is determined by the relative efficiency index $RE = \left(1 + \frac{\lambda_g}{M_g}\right)^{-1}$. A value of M_g is chosen so that RE_g is greater than 90%. The imputation algorithm sequentially iterates through the variables to impute the missing values using $LR_{g,MI}$ fitted on the complete cases as

$$ln\left(\frac{P(X_{g,cc}=1)}{1-P(X_{g,cc}=1)}\right) = \beta_{g0} + \sum_{f=1}^{F} \beta_{gf}\, X_{f,cc}\,, \tag{3.4}$$

where $P(X_{g,cc} = 1)$ is the probability of $X_{g,cc}$ being in level 1, β_{g0} is the model intercept, and β_{gf} are model coefficients. For each X_g, the M_g imputations result in $M_g$logistic regression models, M_g model intercepts, and $M_g \times F$ model coefficients, with differing intercepts and coefficients for each model, collectively defined as β_g.

3.3 Point of Departure

For each variable with missing observations (X_g), the traditional MI technique is based on fitting imputation models M_g times. This procedure results in $M_g$logistic regression models, M_g coefficients (β_g) and hence, M_g imputed datasets. Statistical analysis is then performed on the M_g imputed datasets resulting in M_g statistical model coefficients. Values of the M_g coefficients are pooled into a final result by averaging the coefficient values. While generating M_g imputed datasets ensures variability in the imputed dataset without biasing estimates, pooling the statistical model coefficients results in one set of final statistical model coefficients rather than one set of final imputation model coefficients. Therefore, to obtain one final imputed dataset while maintaining variability, pooling is performed on the M_g imputation model coefficients rather than on the M_g statistical model coefficients. For each X_g, the proposed method is based on fitting imputation models M_g times based on Equation 3.4. The intercepts and coefficients obtained from Equation 3.4 are pooled by averaging over the M_g imputations to calculate the average estimated

intercepts and model coefficients, $\overline{\beta_g}$, as $\overline{\beta_g} = \frac{1}{M_g}\sum_{m_g=1}^{M_g}\beta_{mg}$ where β_{mg} is the estimate of β_g in the m_g^{th} model. Thus, the imputation model $LR_{g,MI}$ is redefined as

$$ln\left(\frac{P(X_{g,cc}=1)}{1-P(X_{g,cc}=1)}\right) = \overline{\beta_{g0}} + \sum_{f=1}^{F}\overline{\beta_{gf}}\,X_{f,cc}\,, \tag{3.5}$$

The model defined in Equation 3.5 is used as the MI imputation model rather than that defined in Equation 3.4. The estimated predictive probability that an individual missing observation $x_{g,miss}$ belongs to level 1 is calculated as

$$P(x_{g,miss}=1) = \frac{\exp\left(\overline{\beta_{g0}}+\sum_{f=1}^{F}\overline{\beta_{gf}}\,X_{f,cc}\right)}{1+\exp\left(\overline{\beta_{g0}}+\sum_{f=1}^{F}\overline{\beta_{gf}}\,X_{f,cc}\right)}\,. \tag{3.6}$$

Predictive probabilities for all missing observations are calculated based on Equation 3.6. If $P(x_{g,miss}=1)$ is greater than 0.5, the missing observation is imputed as level 1; otherwise, it is imputed as level 0.

3.4 Imputation Model Diagnostic and Comparison Approaches

As with any model-based procedure, the fit of the model should be checked using goodness of fit tests (Abayomi et al., 2008), and the subset of the variables to be used in the analysis should be determined (Collins et al., 2001). The model diagnostic approach is based on three criteria and is used to evaluate the fit of the imputation models and to determine the subset of the variables. The three criteria are defined as follows:

1. Satisfaction of variable inflation factor (*VIF*).The *VIF* for X_f is given as $VIF_f = \frac{1}{1-R_f^2}$, where R_f^2 is the coefficient of determination for a multiple regression model, considering X_f is the dependent variable and the remaining X_f variables are the independent variables. A VIF_f greater than 10 indicates that X_f is almost a perfect linear combination of other explanatory variables (i.e., multicollinearity); therefore, the standard errors of the

model coefficients will be inflated. Any correlated variables $(X_{f,corr})$ are not included simultaneously within PMM and MI imputation models.

2. Satisfaction of model requirements (goodness of fit). The Hosmer and Lemeshow test is used to assess goodness of fit based on the chi-square test. Any imputation model with chi-square p-value < 0.05 is rejected.
3. Statistical significance of model parameters. At least one explanatory variable must be significant or the imputation model is rejected.

For each X_g and each imputation technique, logistic regression models are fitted on every combination of X_f resulting in 2 sets of $(2^{X_f} - 1) - D = K$ imputation models $[\text{e.g.}, LR_{gMI} = (LR_{gMI,1}, \dots, LR_{gMI,K})]$ where each LR_{gMI} has M_g imputations. D is the number of models with $X_{f,corr}$. The three criteria defined previously are used to evaluate the 2K models. Models satisfying the three criteria are further evaluated based on the following comparison approach.

From the $N_{g,CC}$ complete cases, missing values are randomly generated by deleting observations of $X_{g,cc}$ so that the percentage of missingness for $X_{g,cc}$ equals that of X_g in the original dataset. The deletion procedure results in G sample datasets with sizes N_{g_s}, and variables X_{g_s} and X_{f_s} with complete and deleted cases defined as $X_{g_s,cc}$ and $X_{g_s,miss}$, respectively. Deleted observations $x_{g_s,miss}$ are imputed using the imputation models defined for T_{PMM} (Equation 3.1) and T_{MI} (Equation 3.5), respectively. For every LR_g that satisfies the three criteria, an error matrix is constructed, where the sum of all frequencies in the matrix is N_{g_s}. Rows (j) of the matrix represent the frequency of the observed class levels for $X_{g_s,miss}$ prior to deletion, and columns (e) represent the frequency of the imputed class levels. The percentage of correctly imputed values, expressed as the cross-classification rate (CCR_{LR_g}), is calculated as

$$CCR_{LR_g} = \frac{\sum_{j=1}^{2} w_{LR_g,jj}}{\sum_{j=1}^{2}\sum_{e=1}^{2} w_{LR_g,je}}, \quad (3.7)$$

where $w_{LR_g,jj}$ represents the number of correctly classified observations found along the diagonal of the error matrix; and the denominator is equal to N_{g_S}. The percentage of each misclassified class, expressed as class error (CE), is calculated as $CE_{LR_g} = 1 - \frac{w_{LR_g,jj}}{\sum_{e=1}^{2} w_{LR_g,je}}$. Balance between CCR and CE is used to choose the "final" imputation model, where models with high CCR values but high CE values are considered less reasonable models for imputing binary variables with missing observations.

3.5 Case Study

A dataset containing observations describing hazard intensities and building attributes for *N*=866 single-family homes in the three counties of coastal Mississippi (Hancock, Harrison, Jackson) that border the Gulf of Mexico is used for the application of the methodology. The continuous variables (X_f) are maximum 3-second gust wind speed ($U_{3,max}$), maximum significant wave height ($H_{S,max}$), maximum surge depth (D_{max}), maximum water speed (U_{max}), and base flood elevations (X_{BFE}). All hazard intensities represent the maximum values of the time series obtained from joint Simulating Waves Nearshore and ADvanced CIRCulation (SWAN+ADCIRC) models (Dietrich et al., 2012) after 2005 Hurricane Katrina. Data for variable X_{BFE} were obtained from the FEMA Flood Map Service Center flood insurance rate maps (FIRMs) for Hancock (1983, 1987, 1992), Harrison, (1980, 1983, 1984, 1988, 2002), and Jackson (1983, 1987, 1992) counties, respectively. The flood maps were georeferenced in ArcGIS and X_{BFE} values were recorded at building footprint locations.

The binary variables with missing data (X_g) are foundation type (FT) and number of stories (NS), where the two levels are defined as (slab, elevated) and (one-story, two-story). Because of

the differences in hazard intensities between counties, it not optimal to use a single county's imputation model to FT and NS in other counties. This may result in a low accuracy of the imputation model; therefore, imputation models were fitted on a county scale. Table 3.1 shows the explanatory variables X_f and the response variable X_g of the imputation models.

Table 3.1 Explanatory and response variables of the dataset used to fit the imputation models in Hancock, Harrison, and Jackson counties

	Symbol	Description	Range (continuous) or Levels (binary)		
			Hancock	Harrison	Jackson
X_f	$U_{3,max}$	Maximum 3-second gust wind speed	(48.57-67.99) m/s	(55.32-67.42) m/s	(47.62-62.54) m/s
	$H_{S,max}$	Maximum significant wave height	(0.3-3.22) m	(0-2.22) m	(0-1.84) m
	D_{max}	Maximum surge depth above local ground level	(0.94-7.94) m	(0-5.96) m	(0-5.18) m
	U_{max}	Maximum water speed	(0.18-2.8) m/s	(0-1.06) m/s	(0-1.45) m/s
	X_{BFE}	Base flood elevation	(0.35-5.23) m	(0.34-4) m	(0.32-4.31) m
X_g	X_{FT}	Foundation type	Slab (0), Elevated (1)		
	X_{NS}	Number of stories	One-Story (1), Two-Story (0)		

Frequency and percentage of observed (η) or missingness (λ) for X_{FT} and X_{NS} are shown in Table 3.2. The missingness patterns of the three datasets were tested and were found to be arbitrary in the three counties. Based on the missingness percentage λ for X_{FT} and X_{NS}, and using a relative efficiency index $RE > 90\%$, the number of required imputations M_g for T_{MI} was calculated as 10. Correlation between $H_{S,max}$ and D_{max} was found to be high, which results in $VIF_{HS,max}$ and VIF_{Dmax} >10. Therefore, $H_{S,max}$ and D_{max} were not included simultaneously in the same imputation models.

Table 3.2 Frequency and percentages of observed (η) or missingness (λ) for X_{FT} and X_{NS} in Hancock, Harrison, and Jackson counties

County	Hancock Frequency (η or λ)	Harrison Frequency (η or λ)	Jackson Frequency (η or λ)	Total
Slab	39 (21%)	86 (23%)	151(50%)	276
Elevated Floor	56 (30%)	130 (34%)	40 (13%)	266
Missing	89 (48%)	163 (43%)	112 (37%)	364
One-Story	26 (14%)	160 (42%)	187 (62%)	373
Two-Story	15 (8%)	39 (10%)	45 (15%)	99
Missing	143 (78%)	180 (47%)	71 (23%)	394

3.5.2 Case Study Imputation Model Diagnostics

For each imputation technique and each county, 23 logistic regression models were fitted. Table 3.3 shows the LR_{g_k} models that satisfied the three diagnostic criteria in each county. Cells with (✓) indicate the variables that are included in each LR_{g_k} models. These models were used to impute X_{FT} and X_{NS} in each county of the study area.

Table 3.3 Imputation models with variables that satisfied the three criteria for X_{FT} and X_{NS} in Hancock, Harrison, and Jackson counties for both T_{PMM} and T_{MI}

	LR_{FT_k}	$U_{3,max}$	$H_{S,max}$	D_{max}	U_{max}	X_{BFE}	LR_{NS_k}	$U_{3,max}$	$H_{S,max}$	D_{max}	U_{max}	X_{BFE}
Hancock	1	✓		✓	✓	✓	1	✓	✓		✓	
	2	✓	✓		✓	✓	2			✓	✓	✓
	3	✓		✓	✓		3		✓		✓	✓
	4	✓	✓		✓		4	✓	✓			✓
	5	✓			✓	✓	5	✓		✓		
	6			✓	✓	✓	6	✓	✓			
	7		✓		✓	✓	7			✓		✓
	8	✓		✓		✓	8			✓		✓
	9	✓	✓			✓	9				✓	✓
	10	✓		✓			10					✓
	11	✓	✓									
	12	✓				✓						
	13			✓	✓							
	14		✓		✓							
	15			✓		✓						
	16		✓			✓						
	17				✓	✓						
	18			✓								
	19		✓									
	20					✓						
Harrison	1			✓	✓	✓	1	✓		✓		✓
	2		✓		✓	✓	2	✓		✓	✓	
	3	✓			✓		3			✓	✓	
	4			✓	✓		4			✓		✓
	5			✓		✓						
	6				✓	✓						
	7				✓							
Jackson	1	✓		✓	✓	✓	1	✓		✓	✓	✓
	2	✓	✓		✓		2	✓	✓		✓	✓
	3	✓		✓	✓		3	✓		✓	✓	
	4	✓	✓		✓		4	✓	✓			
	5	✓			✓	✓	5			✓	✓	✓
	6			✓	✓	✓	6		✓		✓	✓
	7		✓		✓	✓	7	✓		✓		✓
	8	✓		✓		✓	8	✓	✓			✓
	9	✓	✓			✓	9	✓		✓		

Table 3.3 Continued

	LR_{FT_k}	$U_{3,max}$	$H_{S,max}$	D_{max}	U_{max}	X_{BFE}	LR_{NS_k}	$U_{3,max}$	$H_{S,max}$	D_{max}	U_{max}	X_{BFE}
	10	✓		✓			10	✓	✓			
	11	✓	✓				11			✓	✓	
	12			✓	✓		12		✓			
	13		✓		✓		13			✓		✓
	14			✓		✓	14		✓			✓
	15		✓			✓	15			✓		
	16				✓	✓	16		✓			
	17			✓								
	18		✓									
	19				✓							
	20		✓									

From the complete case subdatasets of X_{FT_s} and X_{NS_s} in each county with sample sizes $N_{FT,CC}$ equal to (95, 216, 191) and $N_{NS,CC}$ equal to (41, 199, 232), three sample datasets with sample sizes N_{g_s} are constructed by randomly deleting observations. The observations are deleted so that N_{FT_s} is equal to (46, 93, 71) and N_{NS_s} is equal to (32, 94, 53), which represent equivalent missingness percentages (λ) to those defined in Table 3.2 in each county. The frequency and percentage of observed and missing (λ) cases for X_{FT_s} and X_{NS_s} in the three subdatasets are shown in Table 3.4. The X_{g_s} deleted observations for X_{FT_s} and X_{NS_s} were imputed based on the LR_{g_k} models defined in Table 3.3.

Table 3.4 Percentage of observed η or missingness λ of X_{FT_S} and X_{NS_S} in Hancock, Harrison, and Jackson after observation deletion.

	County	Hancock Frequency (η or λ)	Harrison Frequency (η or λ)	Jackson Frequency (η or λ)
X_{FT}	Observed	49 (52%)	123 (57%)	120 (63%)
	Missing	46 (48%)	93 (43%)	71 (37%)
X_{NS}	Observed	9 (22%)	105 (53%)	179 (77%)
	Missing	32 (78%)	94 (47%)	53 (23%)

3.5.3 Case Study Imputation Model Comparison

Among the models defined in Table 3.3 and for each T and each X_g, one imputation model LR_{g_k} with the highest CCR and the lowest CE was chosen. Error matrix values for LR_{FT_K} and LR_{NS_K} obtained from T_{PMM} and T_{MI} are provided in Tables 3.5 and 3.6, respectively. Rows of the matrices

represent the frequency of slab, elevated foundation, and one- and two-stories prior to deletion, while columns represent the frequency of the imputed binary variable levels after the deletion. The results show that in general the performance of PMM imputation models is higher than that of the MI imputation models, with CCR ranging from 58% to 91%. For X_{FT} in Hancock and Jackson counties, $LR_{FT_{13}}$ and $LR_{FT_{12}}$ models resulting from T_{PMM} have higher $CCR_{LR_{FT}}$ and lower $CE_{LR_{FT}}$ than LR_{FT_2} and $LR_{FT_{12}}$resulting from T_{MI}. In Harrison, T_{MI} model LR_{FT_5} has higher $CCR_{LR_{FT}}$ and lower $CE_{LR_{FT}}$ than of T_{PMM} model LR_{FT_2}. For X_{NS} in Hancock, T_{PMM} model LR_{NS_6} has higher $CCR_{LR_{NS}}$ than that of T_{MI} model LR_{NS_8}. Therefore, LR_{NS_6} was chosen for X_{NS} in Hancock. In Harrison, T_{PMM} model LR_{NS_3} has higher $CCR_{LR_{NS}}$ value and lower $CE_{LR_{NS}}$ than those of T_{MI} model LR_{NS_3} resulting from. Therefore, $LR_{NS_4}$was chosen for X_{NS} in Hancock. In Jackson T_{PMM} model LR_{NS_9} has higher $CCR_{LR_{NS}}$ and lower $CE_{LR_{NS}}$ than those of T_{MI} model LR_{NS_6}. Therefore, $LR_{NS_9}$was chosen for X_{NS} in Jackson. Based on the CCR and CE values, "final" imputation models, shaded in Tables 3.5 and 3.6, are defined for X_{FT} and X_{NS} in each county of the study area.

Equations 3.8 and 3.10 define final T_{PMM} imputation models LR_{13} and LR_{12} for foundation type in Hancock and Jackson counties, respectively, while Equation 3.9 defines the final T_{MI} imputation model (LR_5) for foundation type in Harrison county. These models estimate the probability that buildings with missing foundation data have elevated foundations.

$$ln\left(\frac{P(X_{FT}=\text{Elevated})}{1-P(X_{FT}=\text{Elevated})}\right) = -6.14 + 1.83D_{max} - 2.84U_{max}\ , \tag{3.8}$$

$$ln\left(\frac{P(X_{FT}=\text{Elevated})}{1-P(X_{FT}=\text{Elevated})}\right) = 0.37 - 0.26D_{max} + 0.6X_{BFE}\ , \tag{3.9}$$

$$ln\left(\frac{P(X_{FT}=\text{Elevated})}{1-P(X_{FT}=\text{Elevated})}\right) = -2.86 + 0.29D_{max} + 4.18U_{max}\ . \tag{3.10}$$

Table 3.5 Observed vs. imputed Xg_S error matrices, CE, and CCR for X_{FT_S} in Hancock, Harrison, and Jackson Counties

			Hancock					Harrison					Jackson				
			Imputed X_{g_s}														
T			LR_{FT_K}	Slab	Elevated	$CE_{LR_{FT}}$	$CCR_{LR_{FT}}$	LR_{FT_K}	Slab	Elevated	$CE_{LR_{FT}}$	$CCR_{LR_{FT}}$	LR_{FT_K}	Slab	Elevated	$CE_{LR_{FT}}$	$CCR_{LR_{FT}}$
Observed X_{g_s}	T_{PMM}	Slab	13	20	3	13%	91%	2	23	15	39%	58%	12	49	9	16%	83%
		Elevated		1	22	4%			24	31	44%			3	10	23%	
	T_{MI}	Slab	2	7	16	70%	61%	5	17	21	55%	67%	12	46	12	21%	76%
		Elevated		2	21	9%			10	45	18%			5	8	38%	

Table 3.6 Observed vs. imputed Xg_S error matrices, CE, and CCR for X_{NS_S} in Hancock, Harrison, and Jackson Counties

			Hancock					Harrison					Jackson				
			Imputed X_{g_s}														
T			LR_{NS_K}	One-Story	Two-Story	$CE_{LR_{NS}}$	$CCR_{LR_{NS}}$	LR_{NS_K}	One-Story	Two-Story	$CE_{LR_{NS}}$	$CCR_{LR_{NS}}$	LR_{FT_K}	One-Story	Two-Story	$CE_{LR_{NS}}$	$CCR_{LR_{NS}}$
Observed X_{g_s}	T_{PMM}	One-Story	6	20	0	0%	88%	3	71	2	3%	78%	9	37	8	18%	77%
		Two-Story		4	8	33%			19	2	90%			4	4	50%	
	T_{MI}	One-Story	8	16	4	20%	84%	4	73	0	0%	78%	6	37	8	18%	75%
		Two-Story		1	11	8%			21	0	100%			5	3	63%	

Equations 3.11, 3.12 and 3.13 define the final T_{PMM} imputation models LR_6, LR_3, and LR_9 for number of stories in Hancock, Harrison and Jackson counties, respectively. These models estimate the probability the buildings with missing number of stories data are one-story buildings.

$$ln\left(\frac{P(X_{NS}=\text{One-story})}{1-P(X_{NS}=\text{One-story})}\right) = 24.28 - 0.32U_{3,max} - 5.62H_{S,max}\ , \quad (3.11)$$

$$ln\left(\frac{P(X_{NS}=\text{One-story})}{1-P(X_{NS}=\text{One-story})}\right) = 2.66 + 0.2D_{max} - 6.08U_{max}\ , \quad (3.12)$$

$$ln\left(\frac{P(X_{NS}=\text{One-story})}{1-P(X_{NS}=\text{One-story})}\right) = 5.67 - 0.06U_{3,max} - 0.33D_{max}\ . \quad (3.13)$$

Although the study was restricted to binary missing explanatory variables, LR_{PMM} imputation models performed better than LR_{MI} imputation models in imputing foundation type and number of stories for five of the six models in the three counties of the study area. The missing observations have been imputed as a function of only continuous observed variables (i.e., hazard intensities, base flood elevation) without considering other building attributes; therefore, more observed building attributes in regions that share similar common building construction patterns are needed. Application of the developed approaches on comprehensive datasets will enable stronger evaluation of the performance of imputation models.

3.6 Summary and Conclusions

Imputation model diagnostic and comparison approaches were developed for binary variable imputation techniques. The developed diagnostic approach was used to evaluate the fit of the individual imputation model, while the developed comparison approach was used to evaluate the performance of several imputation models. Logistic regression PMM and MI imputation models were used to impute categorical variables with missing observations based on other continuous observed variables in the dataset. The MI imputation technique was modified to maintain variability resulting from the *M* imputations and to obtain one imputed datasets. A case

study based on a dataset collected in coastal Mississippi after 2005 Hurricane Katrina demonstrated the application of the methodology. Missing foundation type and number of stories for single-family homes were imputed as a function of hazard intensities and base flood elevation. The contributions of this chapter are:

- Development of diagnostic approach for binary categorical variables with missing observations rather than continuous variables with missing observations.
- Development of comparison approach to evaluate the performance of imputation models rather than performance of statistical models fitted on the imputed datasets.
- Maintaining the percentage of missingness and enshrining consistency in fitting and evaluation of the models by developing the comparison approach on dataset with an equivalent missingness percentage to that in the original dataset.
- For the case study, application of the diagnostic and comparison approaches showed an effective approach to evaluate the fit of individual imputation model, and the performance of several imputation models.
- For the case study, the average performance accuracy of PMM imputation models was 9% greater than that of MI models for foundation type.
- For the case study, the average performance accuracy of PMM imputation models was 2% greater than that of MI models for number of stories.

CHAPTER 4. PREDICTIVE DATA-BASED FRAGILITY MODEL FOR SINGLE FAMILY HOMES SUBJECTED TO WIND, WAVE, AND FLOOD HAZARDS CONSIDERING FOUNDATION TYPE AND NUMBER OF STORIES

4.1 Introduction

Data-based fragility models account for a range of variables (Nateghi et al., 2011) that influence building damage, use observed data from similar past events to predict future building damage, and consider variability in building and environmental attributes (Pitilakis et al., 2014). If field data are representative of a range of hazard parameters, building attributes, and building damage data, statistical models will accurately predict damage and identify variables that significantly contribute to damage. External validity, used to assess the performance of statistical models, provides a realistic evaluation of model prediction accuracy. This is an advantage over simulation-based fragility models, as the lack of observed data has been identified as an issue in quantification of model prediction accuracy (Baradaranshoraka et al., 2017; Ellingwood et al., 2004).

Data-based fragility models have been recently implemented to estimate the probability of collapse or being in or exceeding a specified damage state for buildings as a function of hazard parameters (H), and environmental (E) and building attributes (A). Hatzikyriakou and Lin (2018) developed a cumulative logit fragility model to predict the probability of a home being in or exceeding a certain damage state as a function of H (i.e., flood inundation, wave height, dune erosion) and E (i.e., base flood elevation). Hatzikyriakou et al. (2015) developed a component-based logistic regression fragility model to predict the probability of collapse for single-family home foundations, exterior walls, and siding as a function of E (i.e., distance from the coast, ground elevation) and A (i.e., elevation of the lowest horizontal member, structure height above lowest horizontal member, house age, building perimeter). Tomiczek et al. (2014a) developed a

multivariate regression fragility model to estimate the probability of collapse for pile-elevated, wood-framed buildings as a function of H (i.e., maximum significant wave height, breaking wave height, maximum current velocity) and A (i.e., freeboard height, building age). In the previous studies, building damage was modeled as a function of main explanatory variable effects (i.e., H, E, A), where none of the studies discussed above modeled damage as a function of H, E, A main effects and their interactions (e.g., HE, HA, EA). While modeling building damage as a function of main explanatory variables reflects the simultaneous effect of these variables on damage, failure to account for the interactions lead to bias and misinterpretation of the model coefficients. Significant interaction terms reflect variation of the effect of one main explanatory variable on the response variable based on levels of another main explanatory variables (Jaccard & Turrisi, 2003) and must be considered.

Specific to building fragility, Tomiczek et al. (2017) used multiple linear regression to estimate the probability of damage as a function of H (i.e., maximum water velocity, maximum water depth) and A (i.e., minimum freeboard, relative shielding, age), and HA interaction (i.e., maximum water velocity and relative shielding). They found that HA interaction term is an important factor that significantly contributes to damage. Although not specific to buildings, Reed et al. (2016) developed a logit fragility model to predict damage for power systems as a function of H and two (HH) and three (HHH) factor interaction terms, while Kameshwar and Padgett (2018) developed wind buckling and storm surge flotation fragility models for oil storage tanks as a function of H, A and AA interaction terms.

Although previous studies have considered interactions in the development of the fragility models, coefficients of interaction terms have not been interpreted (e.g., through odds ratio), and inference and interpretation have been limited to the indication of the degree of significance.

Interactions between continuous and categorical variables (HA) are easier and more meaningful to interpret than interaction between continuous variables (HH) or between categorical variables (AA); however, HA terms have not been directly modeled and interpreted in the development of data-based building fragility models. When HA terms are statistically significant, they indicate that the effect of H on damage varies for the levels of A; therefore, damage prediction must be based on both main and interaction terms. The contributions of this chapter are the development of data-based fragility models as a function of main hazard parameters (H) and environmental (E) and building attributes (A) effects and the two-factor interaction terms of hazard parameters and building attributes (HA). Additionally, the interpretation of hazard effect on damage is provided based on increased hazard taking into consideration the building attributes. These are advantages over the current data-based building fragility models, where the current models are developed either as a function of main effects, or as a function of main and interactions term effects but without inference and interpretation of the coefficients.

4.1.1 Aim

The aim of Chapter 4 is to develop predictive data-based multi-hazard, hurricane fragility models for single-family homes as a function of continuous variables (H, E), categorical variables (A), and two-factor interaction (HA) of H and A variables. The H variables are maximum 3-second gust wind speed, maximum significant wave height, maximum surge depth, and maximum water speed. The E variable is the FEMA-derived base flood elevation from National Flood Insurance Program (NFIP) Rate Maps ($FIRM_S$). The A variables are foundation type and number of stories imputed from Chapter 3. The HA interactions are the product of H and A variables. Videographic damage and building attribute data recorded in coastal Mississippi after Hurricane Katrina, simulated hazard data computed by the tightly-coupled Simulating WAves Nearshore and ADvanced CIRCulation (SWAN+ADCIRC) model, and base flood elevation values are the model

inputs. Global building damage (i.e., description of the overall building damage) is assessed using the seven-category Wind and Flood (WF) Damage Scale developed by Friedland and Levitan (2009). The models are developed for ordered categorical damage states (DS) and binary collapse/non-collapse, where the probability of being in or exceeding a specified DS and the probability of collapse are estimated using proportional odds cumulative logit and logistic regression models, respectively. Hatzikyriakou et al. (2015), Reed et al. (2016), and Kameshwar and Padgett (2018) all used logistic regression with interaction terms for hurricane damage models, while Reese et al. (2011) used logistic regression without interaction terms for tsunami damage models. Proportional odds cumulative logit models without interaction terms were used by Charvet et al. (2014a), Charvet et al. (2014b), and Charvet et al. (2015) for tsunami damage models, and by Lallemant et al. (2015) and Hatzikyriakou and Lin (2018) for earthquake and hurricane damage models, respectively. Model prediction accuracy is evaluated using external cross-validation (CV), specifically using "leave-one-out" cross-validation (LOOCV) and expressed in terms of the cross-classification rate (CCR).

4.2 Data

4.2.1 Global Building Damage Response Variable

The global building DS response variable (Y) was derived from visual damage assessment of each surveyed building using the Wind and Flood (WF) Damage Scale developed by Friedland and Levitan (2009). Detailed description regarding the damage assessment and aggregation of the global building DS response variable (Y) are presented in Section 2.2.1. Results of the field investigation for 866 single-family homes are presented in Table 4.1. The aggregated Wind and Flood Damage State (WFDS) representing the global building DS response variable Y for n models, each with j levels, $DS_{j,n}$, is presented in Table 4.2.

Table 4.1 Explanatory variables used to construct the fragility models.

Levels, *j*	Damage states	Number of buildings	Percent of buildings
1	WF0=No damage	4	0.46%
2	WF1=Minor damage	7	0.81%
3	WF2=Moderate damage	60	6.96%
4	WF3=Severe damage	349	40.30%
5	WF4=Very severe damage	45	5.20%
6	WF5=Partial collapse	42	4.85%
7	WF6=Collapse	359	41.45%

Table 4.2 Model (*n*), number of observations in each *WFDS*, and global building DS response variable levels for each model, $DS_{j,n}$.

Model (*n*)	WF0	WF1	WF2	WF3	WF4	WF5	WF6
No. Obs.	4	7	60	349	45	42	359
1	$DS_{1,1}$	$DS_{2,1}$	$DS_{3,1}$	$DS_{4,1}$	$DS_{5,1}$	$DS_{6,1}$	$DS_{7,1}$
2	$DS_{1,2}$			$DS_{2,2}$	$DS_{3,2}$	$DS_{4,2}$	$DS_{5,2}$
3	$DS_{1,3}$			$DS_{2,3}$	$DS_{3,3}$	$DS_{4,3}$	
4	$DS_{1,4}$			$DS_{2,4}$		$DS_{3,4}$	
5	$DS_{1,5}$			$DS_{2,5}$		$DS_{3,5}$	$DS_{4,5}$
6	$DS_{1,6}$			$DS_{2,6}$	$DS_{3,6}$		
7	$DS_{1,7}$			$DS_{2,7}$			$DS_{3,7}$
8	$DS_{1,8}$				$DS_{2,8}$	$DS_{3,8}$	$DS_{4,8}$
9	$DS_{1,9}$				$DS_{2,9}$		$DS_{3,9}$
10	$DS_{1,10}$				$DS_{2,10}$	$DS_{3,10}$	
11	$DS_{1,11}$		$DS_{2,11}$	$DS_{3,11}$	$DS_{4,11}$	$DS_{5,11}$	$DS_{6,11}$
12	$DS_{1,12}$		$DS_{2,12}$		$DS_{3,12}$	$DS_{4,12}$	$DS_{5,12}$
13	$DS_{1,13}$		$DS_{2,13}$			$DS_{3,13}$	$DS_{4,13}$
14	$DS_{1,14}$		$DS_{2,14}$				$DS_{,314}$
15	$DS_{1,15}$		$DS_{2,15}$		$DS_{3,15}$		$DS_{4,15}$
16	$DS_{1,16}$		$DS_{2,16}$			$DS_{3,16}$	
17	$DS_{1,17}$		$DS_{2,17}$		$DS_{3,17}$		
18	$DS_{1,18}$		$DS_{2,18}$	$DS_{3,18}$		$DS_{4,18}$	
19	$DS_{1,19}$		$DS_{2,19}$	$DS_{3,19}$			$DS_{4,19}$
20	$DS_{1,20}$		$DS_{2,20}$	$DS_{3,20}$	$DS_{4,20}$		
21	$DS_{1,21}$		$DS_{2,21}$	$DS_{3,21}$	$DS_{4,21}$		$DS_{5,21}$
22	$DS_{1,22}$		$DS_{2,22}$	$DS_{3,22}$		$DS_{4,22}$	$DS_{5,22}$
23	$DS_{1,23}$		$DS_{2,23}$	$DS_{3,23}$	$DS_{4,23}$	$DS_{5,23}$	
24	$DS_{1,24}$	$DS_{2,24}$		$DS_{3,24}$	$DS_{4,24}$	$DS_{5,24}$	$DS_{6,24}$
25	$DS_{1,25}$	$DS_{2,25}$			$DS_{3,25}$	$DS_{4,25}$	$DS_{5,25}$
26	$DS_{1,26}$	$DS_{2,26}$				$DS_{3,26}$	$DS_{4,26}$
27	$DS_{1,27}$	$DS_{2,27}$					$DS_{3,27}$
28	$DS_{1,28}$	$DS_{2,28}$		$DS_{3,28}$		$DS_{4,28}$	
29	$DS_{1,29}$	$DS_{2,29}$		$DS_{3,29}$			$DS_{4,29}$
30	$DS_{1,30}$	$DS_{2,30}$		$DS_{3,30}$			
31	$DS_{1,31}$	$DS_{2,31}$		$DS_{3,31}$	$DS_{4,31}$		$DS_{5,31}$
32	$DS_{1,32}$	$DS_{2,32}$		$DS_{3,32}$	$DS_{4,32}$		
33	$DS_{1,33}$	$DS_{2,33}$		$DS_{3,33}$	$DS_{4,33}$	$DS_{5,33}$	
34	$DS_{1,34}$	$DS_{2,34}$	$DS_{3,34}$		$DS_{4,34}$	$DS_{5,34}$	$DS_{6,34}$
35	$DS_{1,35}$	$DS_{2,35}$	$DS_{3,35}$			$DS_{4,35}$	$DS_{5,35}$

Table 4.2 Continued

Model (n)	WF0	WF1	WF2	WF3	WF4	WF5	WF6
36	$DS_{1,36}$	$DS_{2,36}$	$DS_{3,36}$				$DS_{4,36}$
37	$DS_{1,37}$	$DS_{2,37}$	$DS_{3,37}$				
38	$DS_{1,38}$						$DS_{2,38}$
39	$DS_{1,39}$					$DS_{2,39}$	

4.2.2 Computationally-Modeled Explanatory Hazard Variables

Hazard attributes were characterized using the coupled SWAN +ADCIRC models (Bunya et al., 2010; Dietrich et al., 2010). ADCIRC is tightly coupled with the SWAN model, which evaluating both models to run on the same unstructured mesh and computational cores (Dietrich et al., 2012). Detailed descriptions regarding the simulated hazard variables are presented in Section 2.2.2 and Appendix A.

Table 4.3 lists the continuous explanatory variables (X_h) and (X_{BFE}), and the binary categorical variables (X_a) used to fit the fragility models. Variable X_h are the maximum values of the time series obtained from the coupled SWAN+ADCIRC models.

Table 4.3 Explanatory variables used to construct the fragility models

X_h	Symbol	Description	Range/Levels
x_1	$U_{3.\max}$	Maximum 3-second gust wind speed	[47.63-67.99] m/s
x_2	$H_{S,max}$	Maximum significant wave height	[0-3.20] m
x_3	D_{max}	Maximum surge depth above local ground	[0-7.94] m
x_4	U_{max}	Maximum water speed	[0-2.80] m/s
X_{BFE}		Base flood elevation	[0.32-5.23] m
X_a		Building attributes	Foundation type/Number of stories
X_{FT}	$X_{FT,0}$		Elevated
	$X_{FT,1}$		Slab
X_{NS}	$X_{NS,1}$		One-Story
	$X_{NS,0}$		Two-Story

The maximum surge depth (D_{max}) at the centroid of each building footprint was calculated as the difference between maximum water level (ζ_{max}) and the bathymetry / topography (m) of the SL16 mesh (NAVD88) at that location. Variable X_{BEF} is the base flood elevation (BFE) obtained from the FEMA Flood Map Service Center flood maps for Hancock (1983, 1987, 1992), Harrison,

(1980, 1983, 1984, 1988, 2002), and Jackson (1983, 1987, 1992) counties, respectively. The flood maps were georeferenced in ArcGIS and X_{BFE} values were recorded at building footprint locations.

4.3 Methodology

4.3.1 Fragility Modeling

The generalized forms of binary logistic regression, without and with HA interaction terms, respectively, are given as

$$\text{logit}[P] = \ln\left[\frac{P}{1-P}\right] = \alpha + \sum_{h=1}^{H}\beta_h x_h + \beta_b X_{BFE} + \sum_{a=1}^{A}\beta_a x_a \text{ , and} \quad (4.1)$$

$$\text{logit}[P] = \ln\left[\frac{P}{1-P}\right] = \alpha + \sum_{h=1}^{H}\beta_h x_h + \beta_b X_{BFE} + \sum_{a=1}^{A}\beta_a x_a + \sum_{h=1}^{H}\sum_{a=1}^{A}\beta_{ha}\, x_h x_a \text{ ,} \quad (4.2)$$

where P denotes the probability of collapse; $\text{logit}[P]$ is the logit link function, which is equal to the natural logarithm (log) of the odds of collapse; α is the model intercept; β_h are hazard model coefficients, β_b is base flood elevation model coefficient, β_a are building attribute model coefficients, and β_{ha} are hazard and building attribute interaction term coefficients.

To model the ordered categorical multinomial response (e.g., DS), logistic regression is extended to the proportional odds cumulative logit model, which uses cumulative probabilities to evaluate ordered categories with the proportional odds assumption that curves of the various cumulative logits are parallel. For response variable Y with ordinal levels 1 to J (Table 4.2) and H hazard variables $x_1, x_2, \ldots, x_H$, one E environmental variable (X_{BFE}), and A building attribute variables $x_1, x_2, \ldots, x_A$ (Table 4.3), the log odds of response Y being in level j or greater, without and with HA interactions, respectively, are given for $j \geq 2$ as

$$logit[P(Y \geq j)] = \ln\left[\frac{P(Y \geq j)}{1-P(Y \geq j)}\right] = \alpha_j + \sum_{h=1}^{H}\beta_h x_h + \beta_b X_{BFE} + \sum_{a=1}^{A}\beta_a x_a \text{ , and} \quad (4.3)$$

$$logit[P(Y \geq j)] = \ln\left[\frac{P(Y \geq j)}{1-P(Y \geq j)}\right] = \alpha_j + \sum_{h=1}^{H}\beta_h\, x_h + \beta_b X_{BFE} + \sum_{a=1}^{A}\beta_a x_a +$$

$$\sum_{h=1}^{H}\sum_{a=1}^{A}\beta_{ha}\, x_h x_a \text{ ,} \quad (4.4)$$

where the interactions between building attributes and hazard are represented as the sum of hazard and building attribute product terms "$x_h x_a$." Both Equations 4.3 and 4.4 result in a set of *J – 1* equations with unique intercepts (α_j) and common slopes ($\beta_h, \beta_b, \beta_a, \beta_{ha}$).

To interpret the influence of increasing continuous main effects (i.e., X_h, X_{BFE}) on damage, the specific odds ratios (MOR_h and MOR_{BFE}) for two values of x_h (i.e., x_{h1}, x_{h2}) and X_{BFE} (i.e., x_{BFE1}, x_{BFE2}) with $M_h$unit increase (i.e., where $x_{h2} - x_{h1} = M_h$) and M_{BFE} unit increase (i.e., where $x_{BFE2} - x_{BFE1} = M_{BFE}$), respectively, are calculated as

$$\mathrm{MOR}_{h(1,2)} = \exp[M_h \beta_h)] = \frac{P(Y \geq j | X_h = x_{h1}) / P(Y < j | X_h = x_{h1})}{P(Y \geq j | X_h = x_{h2}) / P(Y < j | X_h = x_{h2})}, \text{ and} \quad (4.5)$$

$$\mathrm{MOR}_{BFE(1,2)} = \exp[M_{BFE} \beta_b] = \frac{P(Y \geq j | X_{BFE} = x_{BFE1}) / P(Y < j | X_{BFE} = x_{BFE1})}{P(Y \geq j | X_{BFE} = x_{BFE2}) / P(Y < j | X_{BFE} = x_{BFE2})}. \quad (4.6)$$

M_h and M_{BFE} are scaling factors that represent multiple or fraction of unit increases in hazard intensities and base flood elevation. $\mathrm{MOR}_{h(1,2)}$ and $\mathrm{MOR}_{BFE(1,2)}$describe the numerical odds of a building being in a higher damage level rather than a lower damage level for each M_h or M_{BFE} unit increase in X_h andX_{BFE}, holding the other variables constant. For logistic regression models $\mathrm{MOR}_{h(1,2)}$ and $\mathrm{MOR}_{BFE(1,2)}$ describe the numerical odds of collapse for each M_h or M_{BFE} unit increase in X_h and X_{BFE}, holding the other variables constant.

To interpret the influence of the categorical binary building attribute levels on damage (i.e., main effects of A), the odds ratio (OR_a) for two levels of x_a (i.e., x_{a0}, x_{a1}) is calculated as

$$\mathrm{MOR}_{a(0,1)} = \exp(\beta_a) = \frac{P(Y \geq j | X_a = x_{a1}) / P(Y < j | X_a = x_{a1})}{P(Y \geq j | X_a = x_{a0}) / P(Y < j | X_a = x_{a0})}. \quad (4.7)$$

$\mathrm{MOR}_{a(0,1)}$ describes the numerical odds of a building being in a higher damage level rather than a lower damage level when a building has level x_{a1} rather than x_{a0} of X_a, holding the other variables constant. For logistic regression models, $\mathrm{MOR}_{a(0,1)}$ describes the numerical odds of collapse when a building has attribute level x_{a1} rather than x_{a0} of X_a, holding the other variables constant. Given

building attributes $X_{a,0}$ and $X_{a,1}$, the odds ratio $\mathrm{MOR}_{ha(1,2)}$ for HA interaction terms is calculated as

$$\mathrm{MOR}_{ha(1,2)} = \exp(M_h \beta_{ha}) . \quad (4.8)$$

This value describes the numerical odds of a building being in a higher damage level rather than a lower damage level for two values of x_h (i.e., x_{h1}, x_{h2}) with M_h unit increase across levels of a building attribute (i.e., $X_{a,0}, X_{a,1}$). For logistic regression models, $\mathrm{MOR}_{ha(1,2)}$ describes the numerical odds of collapse for two values of x_h (i.e., x_{h1}, x_{h2}) with M_h unit increase across levels of a building attribute (i.e., $X_{a,0}, X_{a,1}$). The odds ratio for HA interaction terms also equals the ratio of two odds ratios $\mathrm{MOR}_{h(1,2)}|X_{a,0}$ and $\mathrm{MOR}_{h(1,2)}|X_{a,1}$ and is given as

$$\mathrm{MOR}_{ha(1,2)} = \frac{\mathrm{MOR}_{h(1,2)}|X_{a,1}}{\mathrm{MOR}_{h(1,2)}|X_{a,0}} = \frac{\exp M_h(\beta_h+\beta_{ha})|X_{a,1}}{\exp(M_h\beta_h)|X_{a,0}} = \frac{P(Y\geq j|X_h=x_{h1})/P(Y<j|X_h=x_{h1})|X_{a,1}}{P(Y\geq j|X_h=x_{h2})/P(Y<j|X_h=x_{h2})|X_{a,0}}, \quad (4.9)$$

where $\mathrm{MOR}_{h(1,2)}|X_{a,0}$ is the odds of being in a higher damage level rather than a lower damage level for M_h unit increase of x_h (i.e., x_{h1}, x_{h2}) given building attribute level $X_{a,0}$. $\mathrm{MOR}_{h(1,2)}|X_{a,1}$ is the odds of being in a higher damage level rather than lower damage level for M_h unit increase of x_h (i.e., x_{h1}, x_{h2}) given building attribute level $X_{a,1}$. For logistic regression, $\mathrm{MOR}_{h(1,2)}|X_{a,0}$ is the odds of collapse for M_h unit increase of x_h (i.e., x_{h1}, x_{h2}) given building attributes level $X_{a,0}$. $\mathrm{MOR}_{h(1,2)}|X_{a,1}$ is the odds of collapse for M_h unit increase of x_h (i.e., x_{h1}, x_{h2}) given building attribute level $X_{a,1}$. The 95% lower (LCI) and upper (UCI) confidence intervals ($\mathrm{MOR}_{ha}\mathrm{CI}_{95\%}$) of $\mathrm{MOR}_{ha(1,2)}$ are given as $\exp\left[M_h\left(\hat{\beta}_{ha} \pm 1.96 * \mathrm{SE}(\hat{\beta}_{ha})\right)\right]$. The 95% lower (LCI) and upper (UCI) confidence intervals ($\mathrm{MOR}_h|X_{a,0}\mathrm{CI}_{95\%}$ and $\mathrm{MOR}_h|X_{a,1}\mathrm{CI}_{95\%}$ for $\mathrm{MOR}_{h(1,2)}|X_{a,0}$ and $\mathrm{MOR}_{h(1,2)}|X_{a,1}$, respectively) are given as $\exp\left[M_h\left(\hat{\beta}_h \pm 1.96 * \mathrm{SE}(\hat{\beta}_h)\right)\right]$, and $\exp\left[M_h\left((\hat{\beta}_h + \hat{\beta}_{ha}) \pm 1.96 * \mathrm{SE}(\hat{\beta}_h + \hat{\beta}_{ha})\right)\right]$, respectively, where $\hat{\beta}_h$ are the estimated H coefficients, $\hat{\beta}_{ha}$ are

the estimated HA coefficients, $\mathrm{SE}(\hat{\beta}_h)$ is the standard error of $\widehat{\beta}_h$, and $\mathrm{SE}(\hat{\beta}_h + \hat{\beta}_{ha})$ is the standard error of the summation of $\hat{\beta}_h$ and $\hat{\beta}_{ha}$. The standard error $\mathrm{SE}(\hat{\beta}_h + \hat{\beta}_{ha})$ is calculated as $\sqrt{var(\hat{\beta}_h) + var(\hat{\beta}_{ha}) + 2cov(\hat{\beta}_h, \hat{\beta}_{ha})}$, where $var(\hat{\beta}_h)$ and $var(\hat{\beta}_{ha})$ are the variances of the estimated hazard $(\hat{\beta}_h)$ and estimated building attribute and hazard interaction term coefficients $(\hat{\beta}_{ha})$, respectively, and $cov(\hat{\beta}_h, \hat{\beta}_{ha})$ is the covariance of the estimated hazard coefficients $\hat{\beta}_h$ and HA interaction term coefficients $\hat{\beta}_{ha}$. Values of $var(\hat{\beta}_h)$, $var(\hat{\beta}_{ha})$, and $cov(\hat{\beta}_h, \hat{\beta}_{ha})$ are obtained from the variance-covariance matrix of the model coefficients.

4.3.2 Model Fitting and Evaluation

To model the interaction terms based on Equations 4.2 and 4.4, each Model (*n*) was first fitted with main effects based on Equations 4.1 and 4.3. Three rejection criteria for screening purposes and to further narrow the net are used to evaluate the fit of these models. For each Model (*n*), three sets of models (*S*, *F*, and *K*) were fitted. Models (*S*) consist of 21 model combinations described in Table 4.4, where (✓) indicates the main explanatory variables included in the models. These models are described as: 1) one model with 6 main explanatory variables, 2) models with combinations of 5 main explanatory variables, and 3) models with combinations of 4 main explanatory variables. Variable $H_{d,max}$ describes the wave depth above local ground and is calculated as $(H_{S,max} + D_{max}) - h$, where h is approximate first floor elevation of each house in meters. Approximate first floor elevation was calculated as the sum of the top of the lowest floor height above local ground and topography at that location, where the top of lowest floor height above local ground was estimated by counting the number of building steps and assuming an average 17.8 cm (7 inch) step rise. The fit of the *S* models resulted in 819 models.

Table 4.4 The *S* model combinations with main explanatory variables

S	$U_{3,max}$	$H_{d,max}$	U_{max}	X_{BFE}	X_{FT}	X_{NS}
1	✓	✓	✓	✓	✓	✓
2		✓	✓	✓	✓	✓
3	✓		✓	✓	✓	✓
4	✓	✓		✓	✓	✓
5	✓	✓	✓		✓	✓
6	✓	✓	✓	✓		✓
7	✓	✓	✓	✓	✓	
8			✓	✓	✓	✓
9		✓		✓	✓	✓
10		✓	✓		✓	✓
11		✓	✓	✓		✓
12		✓	✓	✓	✓	
13	✓			✓	✓	✓
14	✓		✓		✓	✓
15	✓		✓	✓		✓
16	✓		✓	✓	✓	
17	✓	✓			✓	✓
18	✓	✓		✓		✓
19	✓	✓		✓	✓	
20	✓	✓	✓			✓
21	✓	✓	✓		✓	

Models (*F*) consist of 21 model combinations described in Table 4.5, where (✓) indicates the main explanatory variables included in the models These models are described as: 1) one model with 6 main explanatory variables, 2) models with combinations of 5 main explanatory variables, and 3) models with combinations of 4 main explanatory variables. Variable $D_{W,max}$ describes the surge depth within the building and is calculated as the difference between surge depth (D_{max}) and *h*. The fit of the *F* models resulted in 819 models.

Table 4.5 The *F* model combinations with main explanatory variables

F	$U_{3,max}$	$D_{W,max}$	U_{max}	X_{BFE}	X_{FT}	X_{NS}
1	✓	✓	✓	✓	✓	✓
2		✓	✓	✓	✓	✓
3	✓		✓	✓	✓	✓
4	✓	✓		✓	✓	✓
5	✓	✓	✓		✓	✓
6	✓	✓	✓	✓		✓
7	✓	✓	✓	✓	✓	
8			✓	✓	✓	✓
9		✓		✓	✓	✓
10		✓	✓		✓	✓

Table 4.5 Continued

F	$U_{3,max}$	$D_{W,max}$	U_{max}	X_{BFE}	X_{FT}	X_{NS}
11		✓	✓	✓		✓
12		✓	✓	✓	✓	
13	✓			✓	✓	✓
14	✓		✓		✓	✓
15	✓		✓	✓		✓
16	✓		✓	✓	✓	
17	✓	✓			✓	✓
18	✓	✓		✓		✓
19	✓	✓		✓	✓	
20	✓	✓	✓			✓
21	✓	✓	✓		✓	

Models (K) consist of 13 model combinations described in Table 4.6, where (✓) indicates the main explanatory variables included in the models. These models are described as: 1) two models with 6 main explanatory variables, and 2) models with combinations of 5 main explanatory variables. The combinations of 5 and 6 variables were chosen so that the majority of hazard and building attribute variables are included in the fragility models. The fit of the K models resulted in 507 models.

Table 4.6 The K model combinations with main explanatory variables

K	$U_{3,max}$	D_{max}	U_{max}	X_{BFE}	$H_{S,max}$	X_{FT}	X_{NS}
1	✓		✓	✓	✓	✓	✓
2	✓	✓	✓	✓		✓	✓
3			✓	✓	✓	✓	✓
4		✓	✓	✓		✓	✓
5	✓		✓	✓		✓	✓
6	✓			✓	✓	✓	✓
7	✓	✓		✓		✓	✓
8	✓		✓		✓	✓	✓
9	✓	✓	✓			✓	✓
10	✓		✓	✓	✓		✓
11	✓	✓	✓	✓			✓
12	✓		✓	✓	✓	✓	
13	✓	✓	✓	✓		✓	

The three rejection criteria are used to evaluate the fit of the three model sets with main explanatory variables. These criteria are described as following:

1. Satisfaction of model requirements (proportional odds assumption and goodness of fit).

   For proportional odds cumulative models, the proportional odds assumption assumes that

the coefficients for each predictor must be equal across all DS levels and is tested using the chi-square test. For the logistic regression model, the Hosmer and Lemeshow test is used to assess goodness of fit based on the chi-square test. Any model with chi-square *p*-value < 0.05 is rejected.

2. Statistical significance of model parameters. At least one main explanatory variable must be significant or the model is rejected.
3. Reasonableness of response variable model. Models with unreasonable response variable grouping (e.g., minor damage falls into the same level as severe damage) are considered less reasonable models for damage prediction and excluded from further consideration.

Among the three model sets, models satisfying Criterion 1 are evaluated for Criteria 2 and 3. Models satisfying the three criteria are then refitted based on Equations 4.2 and 4.4 to include interactions and are re-evaluated based on Criterion 1. Models with interaction terms are described as models with main explanatory variables (H, E, A) and HA interactions. In addition to Criterion 1, two other criteria are used to evaluate the fit and prediction of the models with interaction terms. These two criteria are described as:

A. Statistical significance of model parameters. All interaction terms included in the model must be significant or the model is rejected.

   Balance between CCR and class error. Once models that pass Criteria 1and A are identified, this criterion is used to evaluate the most reasonable model(s) for prediction. Models with high prediction accuracy (i.e., high value of CCR) but with high class error (i.e., high value of CE) are considered less reasonable models for damage prediction.

4.4 Model Validation

Prediction accuracy for logistic regression and proportional odds cumulative logit models is evaluated using leave-one-out cross-validation (LOOCV). Detailed description regarding model validation is presented in Section 2.5.

4.5 Results

4.5.1 Fragility Fitting

Table 4.7 describes the variables used to fit the models that satisfy Criteria 1 and 2. The remainder of the models failed to meet Criterion 1 and were not further tested for Criterion 2. Models 9, 26, 27, 30 and 37 were fitted based on Equation 4.3, and Model 38 was fitted based on Equation 4.2.

Table 4.7 Models with main explanatory variables that satisfied Criteria 1 and 2

Model (n)	$U_{3,max}$	U_{max}	X_{BFE}	$H_{S,max}$	X_{FT}	X_{NS}
9	✓	✓		✓	✓	✓
26		✓	✓	✓	✓	✓
	✓	✓		✓	✓	✓
27		✓	✓	✓	✓	✓
	✓	✓		✓	✓	✓
	✓		✓	✓	✓	✓
30		✓	✓	✓	✓	✓
	✓	✓		✓	✓	✓
37	✓	✓	✓		✓	✓
38	✓	✓		✓	✓	✓

These models were further evaluated based on Criterion 3. Models 26 and 27 have an unreasonable grouping, with $DS_{2,26}$ and $DS_{2,27}$ ranging from minor damage to very severe damage and partial collapse, respectively, Model 30 has an unreasonable grouping, with $DS_{3,30}$ ranging from severe damage to collapse, and Model 37, has an unreasonable grouping, with $DS_{3,37}$ ranging from moderate damage to collapse.

Because of the unreasonable DS groupings, Models 26, 27, 30, and 37 were excluded from further consideration. To include HA interactions, Models 9, and 38 were refitted based on

Equations 4.2 and Equation 4.4, respectively. Models 9, and 38, with variables described in Table 4.8, satisfied Criteria 1 and A.

Table 4.8 Models with main explanatory variables and interaction effects that satisfied Criteria 1 and A

Model (n)	$U_{3,max}$	U_{max}	$H_{S,max}$	X_{FT}	X_{NS}	$H_{S,max} * X_{NS}$
9	✓	✓	✓	✓	✓	✓
38	✓	✓	✓	✓	✓	✓

Table 4.9 contains the estimated coefficients, standard error, p-value, factored model coefficients ($M_h\beta_h$, $M_h\beta_{ha}$), MOR_h, MOR_{ha} (calculated from Equation 4.8), and corresponding LCI and UCI ($MOR_hCI_{95\%}$ and $MOR_{ha}CI_{95\%}$) for models that met Criteria 1 and A.

Table 4.9 Parameter estimates, standard error, p-value, MOR_h, MOR_{ha}, $MOR_hCI_{95\%}$, and $MOR_{ha}CI_{95\%}$ for models satisfying Criteria 1 and A.

Model	Coefficient	Parameter	Estimated	Std. Error	p-value	$M_h\beta_h$ or $M_h\beta_{ha}$	MOR_h or MOR_{ha}	$MOR_hCI_{95\%}$ or $MOR_{ha}CI_{95\%}$	
								LCI	UCI
9	$\hat{\alpha}_2$	Intercept 2	-6.17	1.68	<0.0001*	-	-	-	-
	$\hat{\alpha}_3$	Intercept 3	-7.03	1.68	0.0002*	-	-	-	-
	$\hat{\beta}_1$	$U_{3,\max}$	0.05	0.03	0.0899	0.23	1.25	0.96	1.63
	$\hat{\beta}_2$	U_{max}	1.42	0.66	0.0321*	0.71	2.03	1.07	3.88
	$\hat{\beta}_3$	$H_{S,\max}$	2.71	0.44	<0.0001*	0.81	2.25	1.74	2.92
	$\hat{\beta}_4$	X_{FT}	0.48	0.18	0.0079*	-	1.62	1.14	2.30
	$\hat{\beta}_5$	X_{NS}	-2.55	0.69	0.0002*	-	0.08	0.02	0.30
	$\hat{\beta}_6$	$H_{S,\max}X_{NS}$	2.22	0.57	<0.0001*	0.67	1.95	1.39	2.72
38	$\hat{\alpha}$	Intercept	-7.92	2.17	0.0003*	-	-	-	-
	$\hat{\beta}_1$	$U_{3,\max}$	0.06	0.03	0.1042	0.27	1.31	1.01	1.71
	$\hat{\beta}_2$	U_{max}	1.06	0.72	0.1428	0.53	1.7	0.84	3.44
	$\hat{\beta}_3$	$H_{S,\max}$	2.90	0.51	<0.0001*	0.87	2.39	1.77	3.22
	$\hat{\beta}_4$	X_{FT}	0.72	0.21	0.0008	0.72	2.05	1.36	3.1
	$\hat{\beta}_5$	X_{NS}	-3.13	0.91	0.0006	-3.13	0.04	0.01	0.26
	$\hat{\beta}_6$	$H_{S\max}X_{NS}$	2.68	0.74	0.0002	0.80	2.23	1.45	3.45

* Significant at α= 0.05

Factored model coefficients, MOR_h, and $MOR_hCI_{95\%}$ were calculated using $M_{U_{3,\max}} = 4.5$ (m/s), $M_{H_{S,\max}} = 0.3$ (m), and $M_{U_{max}} = 0.5$ (m/s). Asterisks appearing after p-values denote statistically significant parameters at $\alpha = 0.05$ level.

4.5.2 Interpretation of Main Effects of DS and Collapse Fragility Models

For Model 9, the results show that the damage of buildings subjected to wind, wave, and water speed are significantly affected by the maximum significant wave height wave and maximum water speed. Maximum 3-second wind speed was found not to be a significant variable that contribute to damage. As maximum significant wave height increase, the odds of being in a higher DS are greater for one-story buildings than for two-story building. No significant interactions were found for number of stories with wind speed or water speed. No significant interactions were found for foundation type with any of the hazard variables. Interpretation of the odds for water speed and foundation main effects for Model 9 signifies that holding all other variables constant:

- for every 0.5 m/s (1.12 mph) increase in maximum water speed, the odds of being in a higher DS are 2.03 times greater (103% increase in odds).
- for buildings with slab foundations, the odds of being in a higher DS are 1.62 times greater (62% increase in odds) than for building with elevated foundations.

For the logistic model, the results show that the collapse potential of buildings subjected to wind, wave, and water speed is significantly affected by only maximum significant wave height. Interpretation of the odds for foundation main effect signifies that holding all other variables constant:

- for buildings with slab foundations, the average odds of collapse are 2.05 times greater (105% increase) than for buildings with elevated foundations.

4.5.3 Interpretation of Interaction Terms of DS and Collapse Fragility Models

Figures 4.1 a), and b) show estimated odds $\text{MOR}_h|X_{a,1}$, $\text{MOR}_h|X_{a,0}$ (i.e., numerator and denominator of Equation 4.9) and the LCI and UCI for Models 9 and 38, respectively. The ratio of $\text{MOR}_h|X_{a,0}$ and $\text{MOR}_h|X_{a,1}$ is equal to the MOR_{ha} shown in Table 4.9.

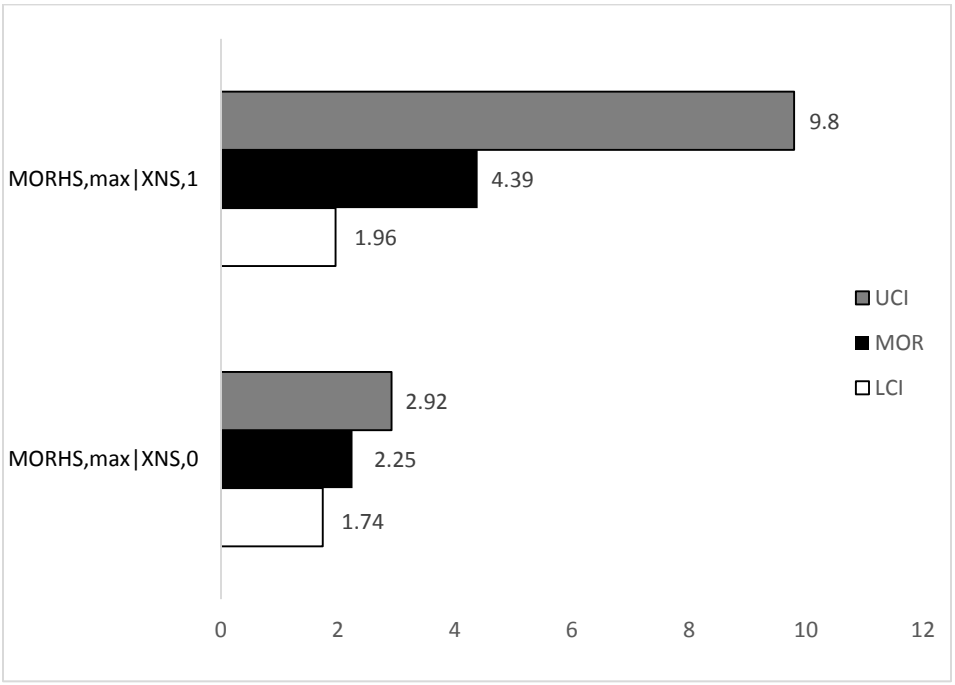

a)

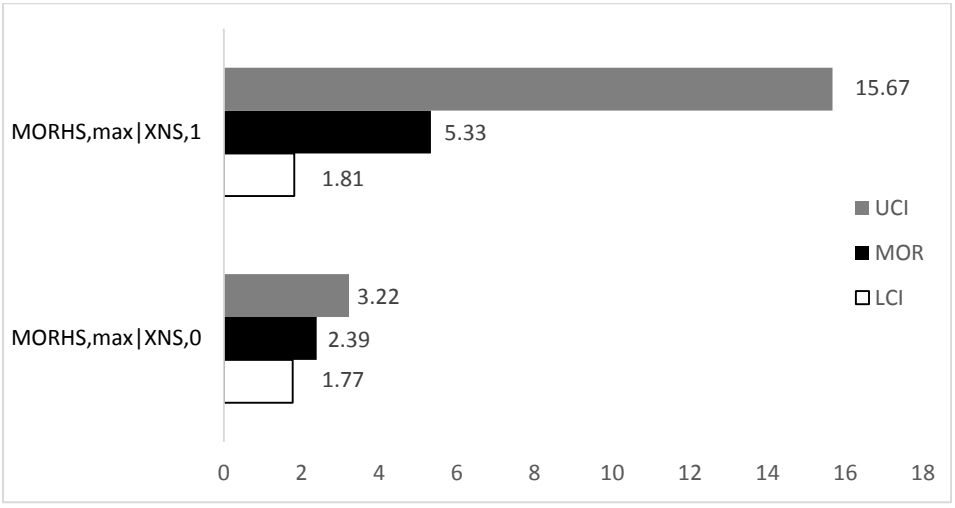

b)

Figure 4.1 Estimated odds $\text{MOR}_h|X_{a,0}$, $\text{MOR}_h|X_{a,1}$, and LCI and UCI for a) Model 9, and b) Model 38.

For Model 9, interpretation of the odds for the interaction terms signifies that, holding all other variables constant:

- The odds ratio $\mathrm{MOR}_{HS,\max,X_{NS}}$ (Table 4.9) for interaction of maximum significant wave height and number of stories is 1.95. This is interpreted as: for every 0.3 m (1.98 ft) increase in maximum significant wave height, the odds of being in a higher DS are 1.95 times greater for one-story buildings (4.39) rather than two-story buildings (2.25) (Figure 4.1a).

For Model 38, interpretation of the odds for the interaction terms signifies that, holding all other variables constant:

- The odds ratio $\mathrm{MOR}_{H_{S,\max},X_{NS}}$ (Table 4.9) for interaction of maximum significant wave height and number of stories is 2.23. This is interpreted as: for every 0.3 m (1.98 ft) increase in maximum significant wave height, the odds of collapse are 2.23 times greater for one-story buildings (5.33) rather than two-story buildings (2.39) (Figure 4.1b).

4.5.4 Model Validation and Evaluation

LOOCV error matrices for Models 9, and 38 are provided in Table 4.10. Rows of the table represent the frequency of observed DS, while columns represent the frequency of predicted DS $\left(\widehat{DS}\right)$. The *n* subscript in the predicted DS $\left(\widehat{DS}_n\right)$ represents the corresponding model number.

Table 4.10 Observed vs. predicted model error matrices, CE, and CCR for non-rejected models

$DS_{j,n}$	$\widehat{DS}_{1,n}$	$\widehat{DS}_{2,n}$	$\widehat{DS}_{3,n}$	Observed Sum	CE	CCR
$DS_{1,9}$	383	14	23	420	8%	84%
$DS_{2,9}$	41	9	37	87	89%	
$DS_{3,9}$	19	9	331	359	7%	
$DS_{1,38}$	468	39	--	507	7%	90%
$DS_{2,38}$	45	314	--	359	13%	

Note: -- indicates error terms are not applicable due to the number of damage levels *j* for model *n*.

Model 9 predicts probability of being in of exceeding damage state with 84% prediction accuracy as a function of maximum 3-second gust wind speed, maximum water speed, maximum significant wave height, foundation type, number of stories, and interaction of number of stories with maximum significant wave height. Model 9 show 3% increased prediction accuracy in comparison to models fitted with only hazard parameters (Chapetr2). The CE values $DS_{1,9,}$ and $DS_{3,9}$ decreased by 4% and the CE value $DS_{2,9}$ increased by 4% in comparison to model fitted with only hazard parameters. The estimated probability of being in or exceeding $DS_{2,9}$ and $DS_{3,9}$, respectively, is estimated as

$$logit\left[P(Y \geq \mathrm{DS}_{2,9})\right] = -6.17 + 0.05 * U_{3,\max} + 1.42 * U_{max} + 2.71 * H_{S,\max} + 0.48 * X_{FT} - 2.55 * X_{NS} + 2.22 * H_{S,\max}X_{NS}, \text{ and} \quad (4.10)$$

$$logit\left[P(Y \geq \mathrm{DS}_{3,9})\right] = -7.03 + 0.05 * U_{3,\max} + 1.42 * U_{max} + 2.71 * H_{S,\max} + 0.48 * X_{FT} - 2.55 * X_{NS} + 2.22 * H_{S,\max}X_{NS}\ . \quad (4.11)$$

Figures 4.2, 4.3. 4.4, and 4.5 show fragility surfaces for Model 9 as a function of maximum significant wave height and maximum water speed. The surfaces are for one- and two-story buildings with elevated and slab foundations subjected to 62 m/s maximum 3-second wind speed.

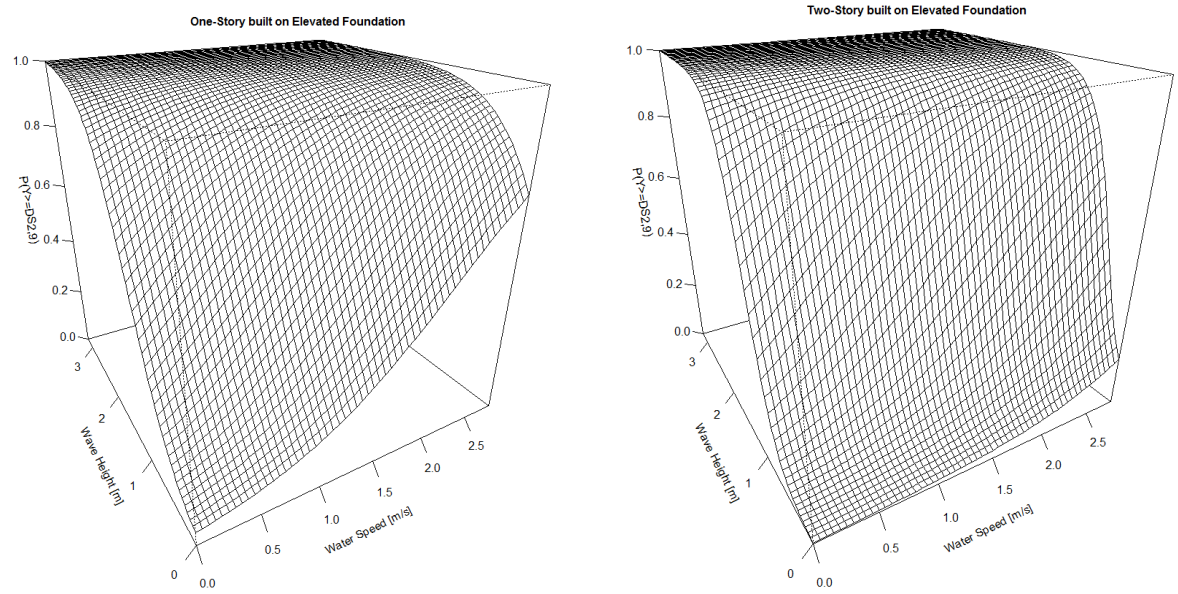

a) b)

Figure 4.2 Probability of being in or exceeding $DS_{2,9}$ for a) one-story built on elevated foundation, and b) two-story built on elevated foundation as a function of maximum significant wave height and maximum water speed.

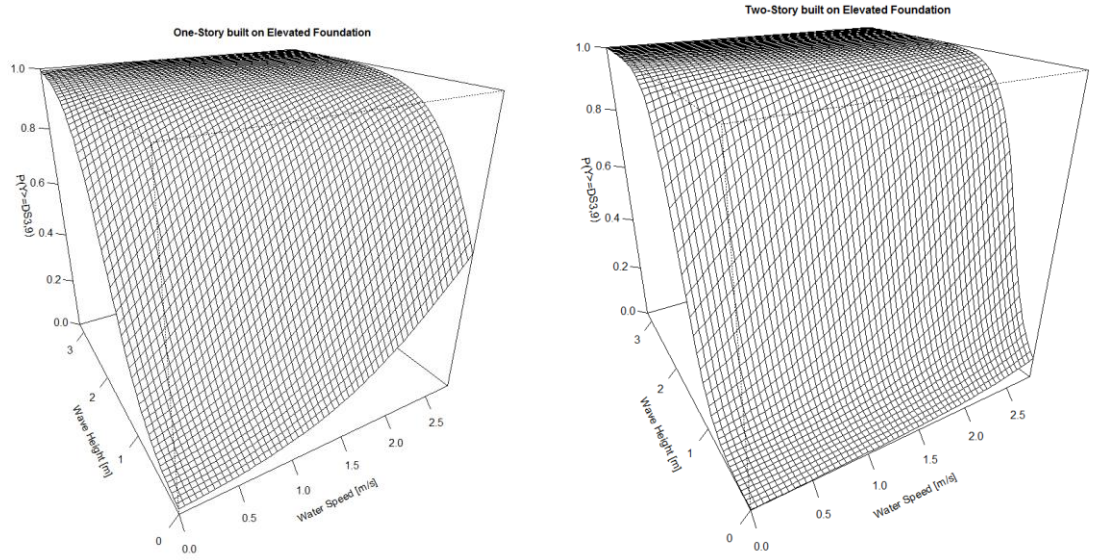

a) b)

Figure 4.3 Probability of being in or exceeding $DS_{3,9}$ for a) one-story built on elevated foundation, and b) two-story built on elevated foundation as a function of maximum significant wave height and maximum water speed.

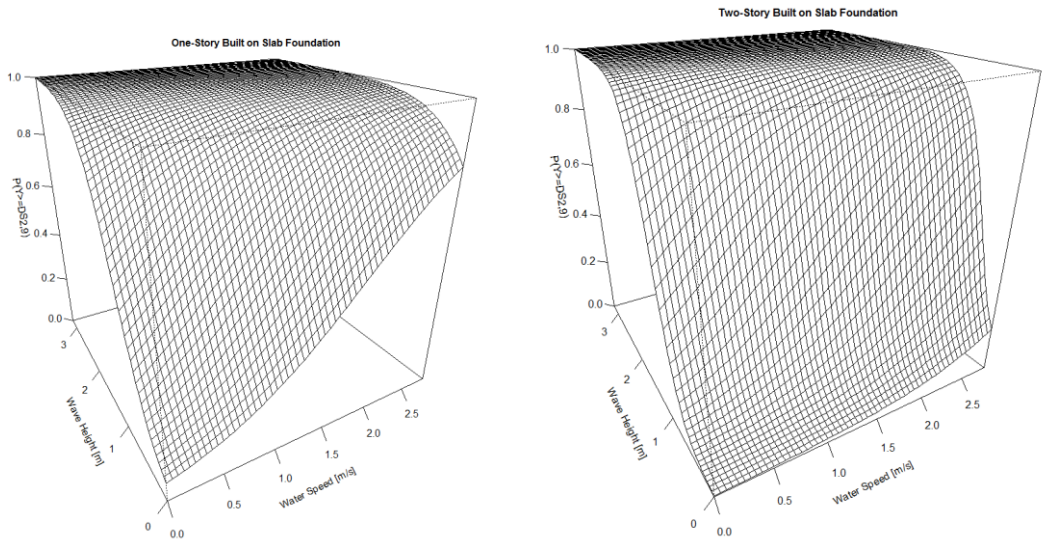

a) b)

Figure 4.4 Probability of being in or exceeding $DS_{2,9}$ for a) one-story built on slab foundation, and b) two-story built on slab foundation as a function of maximum significant wave height and maximum water speed.

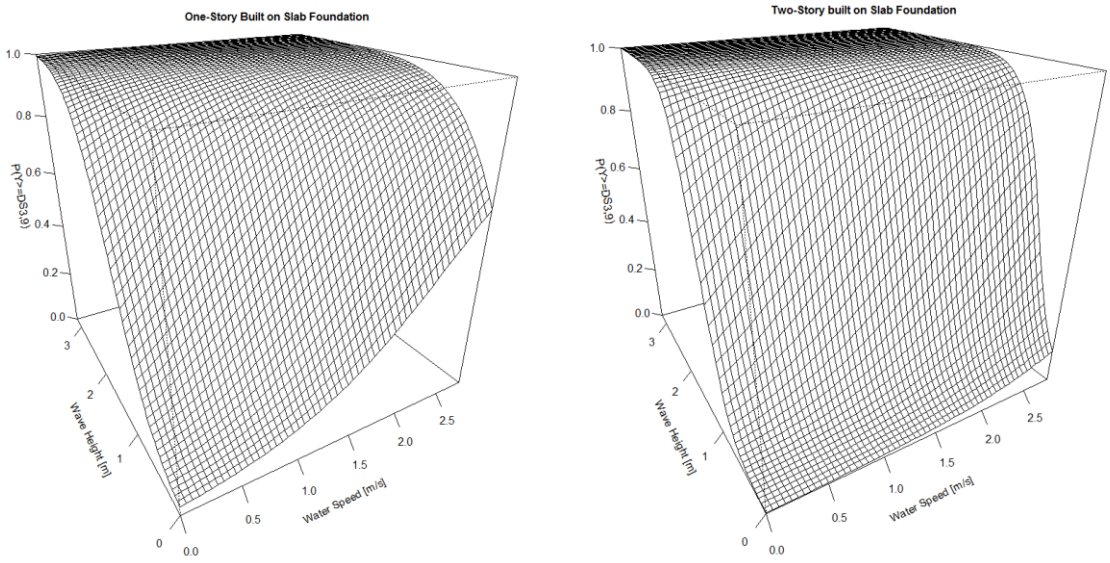

a) b)

Figure 4.5 Probability of being in or exceeding $DS_{3,9}$ for a) one-story built on slab foundation, and b) two-story built on slab foundation as a function of maximum significant wave height and maximum water speed.

Model 38 predicts probability of collapse with 90% prediction accuracy as a function of maximum 3-second gust wind speed, maximum water speed, maximum significant wave height, foundation type, number of stories, and interaction of number of stories with maximum significant wave height. Model 38 shows 3% increase in prediction accuracy, and 4% and 3% decrease in CE for $DS_{1,38}$ and $DS_{2,38}$, respectively, in comparison to the model fit with only hazard parameters. The estimated probability of collapse is given as

$$logit\left[P(Y \geq \mathrm{DS}_{38,2})\right] = -7.92 + 0.06 * U_{3,\max} + 1.06 * U_{max} + 2.90 * H_{\mathrm{S,max}} + 0.72 * X_{FT} - 3.13 * X_{NS} + 2.68 * H_{\mathrm{S,max}} X_{NS} \,. \quad (4.12)$$

Figures 4.6, and 4.7 show fragility surfaces for Model 38 as a function of maximum significant wave height and maximum water speed. The surfaces are for one- and two-story building with elevated and slab foundations subjected to 62 m/s maximum 3-second wind speed.

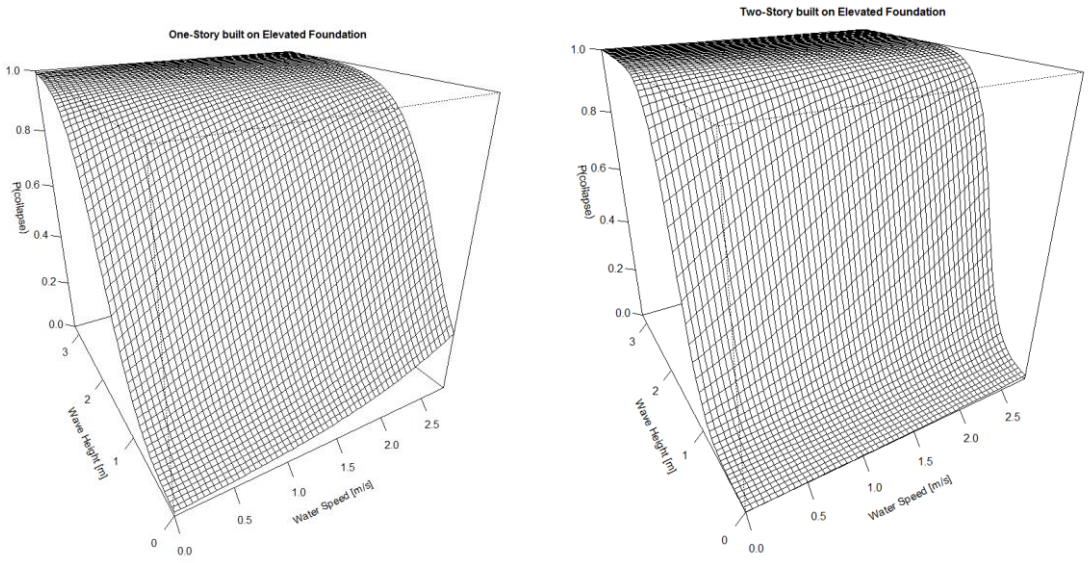

a) b)

Figure 4.6 Probability of collapse for a) one-story built on elevated foundation, and b) two-story built on elevated foundation as a function of maximum significant wave height and maximum water speed.

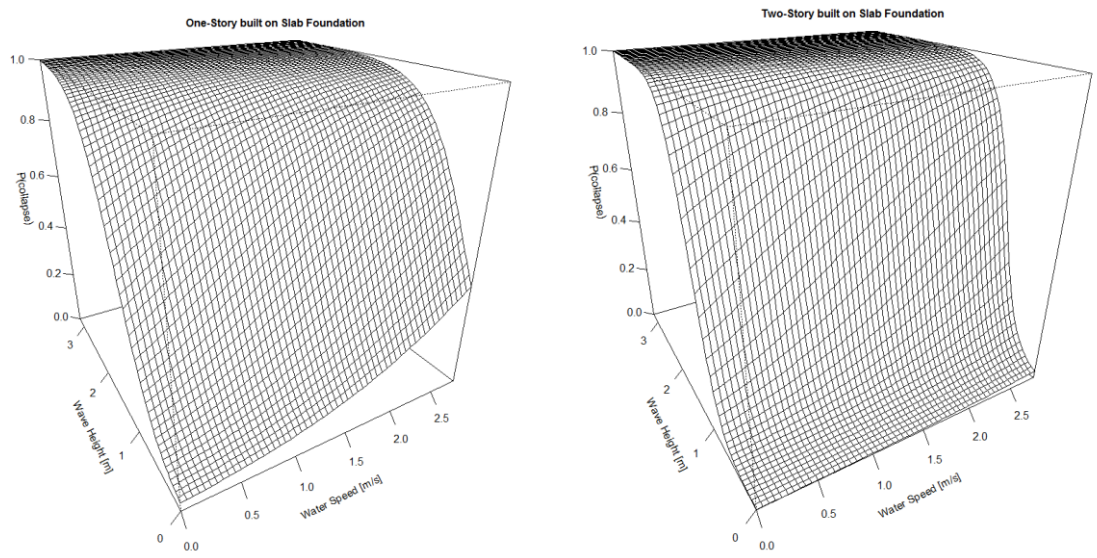

a) b)

Figure 4.7 Probability of collapse for a) one-story built on slab foundation, and b) two-story built on slab foundation as a function of maximum significant wave height and maximum water speed.

4.6 Discussion

Although the overall prediction accuracy of the models fit with the addition of building attributes and interaction terms did not greatly increase in comparison to those fit with only hazard parameters (Chapter 2), interaction of maximum significant wave height with number of stories was statistically significant and showed that damage for one-story buildings increases significantly than for two-story buildings with increasing wave height. The interaction of number of stories and maximum significant wave height was significant in the DS and collapse models. No significant interaction terms for foundation type with any hazard parameters were found. Both DS and collapse models showed that regardless of hazard type, buildings with slab foundations had more damage than elevated buildings. The BFE variable was not shown to be a predictor for damage and collapse because either the models with BFE did not satisfy Criterion 1, or the BFE variable was not significant.

4.7 Summary and Conclusions

Physical damage to one- and two-story residential buildings with slab and elevated foundations was statistically modeled as a function of hurricane wind, wave, and storm surge hazards. Interaction terms that describe the effect of hurricane hazard parameters on damage and collapse based on building attribute variables were modeled and interpreted. The proportional odds cumulative logit and logistic regression models were used to estimate the probability of being in or exceeding DS and the probability of collapse, respectively. The probability of being in or exceeding ordered categorical DS and the probability of collapse were estimated as a function of maximum 3-second gust wind speed, maximum significant wave height, maximum surge depth, maximum water speed, foundation type, number of stories, and two-factor interactions of hazard and building attribute variables. The findings of this chapter are:

- Maximum water speed, and maximum significant wave height were found to be significant hazard predictors of damage for the ordered categorical DS models, while maximum significant wave height was found to be significant hazard predictors for collapse.
- Foundation type and number of stories were found to be significant building attribute predictors for damage and collapse.
- One-story buildings are 1.95 times more likely to be in a higher damage state than two-story buildings for every 0.3 m increase in maximum significant wave height.
- One-story buildings are 2.23 times more likely to collapse than two-story buildings for every 0.3 m increase in maximum significant wave height.
- No significant interactions were found between hazard and foundation type for ordered categorical DS and collapse models.

- Regardless of hazard type, buildings with slab foundations are 1.62 times more likely to be in a higher damage state than elevated buildings.
- Regardless of the hazard type, buildings with slab foundations are 2.05 times more likely to collapse than elevated buildings.

CHAPTER 5. CONCLUSIONS AND RECOMMENDATIONS

5.1 Introduction

The overarching goal of this dissertation research was to improve data-based damage prediction for residential construction subjected to multi-hazard hurricane hazards at the individual building scale. In order to address the overarching goal, three objectives were identified:

- Develop predictive data-based hurricane building (i.e., global) fragility models as functions of hurricane hazard parameters and their interactions.
- Develop diagnostic and comparison approaches to evaluate the performance of binary variable imputation models used to maximize use of aftermath datasets with missing building attribute data.
- Develop predictive data-based hurricane building (i.e., global) fragility models as functions of hurricane hazard parameters, building attributes, and their interactions.

Chapters 2 through 4 described the work accomplished to achieve these objectives and summaries of the work and findings for each of the objectives were presented at the end of each chapter. Chapter 5 discusses conclusions of the three objectives and explains how each objective is applied to model single family home fragility for hurricane multi-hazard events.

5.2 Predictive Data-Based Fragility Model for Single Family Homes Subjected to Wind, Wave, and Flood Hazards

General deficiencies within current data-based hurricane fragility models are the inappropriate use of modeling approaches for multinomial and binomial responses and absence of model performance evaluation for future damage prediction. The aim of Chapter 2 was to develop predictive data-based fragility models for ordered categorical damage states (DS) and binary collapse/non-collapse as a function of hurricane hazard parameters and their interactions. Proportional odds cumulative logit and logistic regression models were used to develop the

fragility models. The probability of buildings being in or exceeding a specified DS and the probability of collapse was estimated using proportional odds cumulative logit and logistic regression models, respectively. External cross-validation (CV), using "leave-one-out" cross-validation (LOOCV) was performed to evaluate model prediction accuracy.

The results of Chapter 2 provide effective statistical models to predict damage and collapse of buildings subjected to simultaneous hurricane hazards. Additionally, results provide a practical approach to identify hazard variables that significantly contribute to damage and collapse. Contributions of Chapter 2 are the development of predictive damage and collapse models as a function of more than one hazard, identification of hazard variables that significantly contribute to damage and collapse, and validation of model prediction accuracy.

5.3 Diagnostic and Comparison Approaches for Logistic Regression Imputation Models

A general deficiency in current imputation model diagnostic and comparison approaches is the absence of numerical diagnostic and comparison approaches for binary variable imputation models. The aim of Chapter 3 was to develop diagnostic and comparison approaches to evaluate the performance of imputation models for binary categorical building attributes with missing observations. Two model-based imputation models, defined as predictive mean matching (PMM) and multiple imputation (MI), were used to impute building attributes with missing obviations. A novel diagnostic approach based on the logistic regression goodness of fit test and significance of model parameters was developed to evaluate the fit of each imputation model. A comparison approach based on finding the percentage of correctly imputed observations, expressed in terms of cross-classification rate (CCR) was developed to compare the performance of the PMM and MI imputation models.

The results of Chapter 3 provide a novel approach to diagnose and compare binary categorical variable imputation models. The contributions of Chapter 3 are the development of a

binary variable numerical diagnostic approach and development of an imputation model comparison approach that is applicable to the imputation model rather than to the statistical model fit on the imputed data.

5.4 Predictive Data-Based Fragility Model for Single Family Homes Subjected to Wind, Wave, and Flood Hazards Considering Foundation Type and Number of Stories

General deficiencies within current hurricane data-based fragility models, which are a function of hazard parameters and building attributes, include lack of consideration and interpretation of interaction terms between hazard parameters and building attribute variables, and absence of model performance evaluation for future damage prediction. The aim of Chapter 4 was to develop predictive data-based fragility models for ordered categorical damage states (DS) and binary collapse/non-collapse as a function of hazard parameters (H), building attributes (A), and two-factor interactions (HA) of hazard parameters and building attributes. The probability of buildings being in or exceeding a specified DS and the probability of collapse are estimated using proportional odds cumulative logit and logistic regression models, respectively. External cross-validation (CV), specifically using "leave-one-out" cross-validation (LOOCV) is performed to evaluate model prediction accuracy.

The results of Chapter 4 provide effective statistical models to predict damage and collapse for residential one- and two-story buildings with slab and elevated foundations subjected to simultaneous hurricane hazards. Additionally, results provide a practical approach to identify hazard and building variables that significantly contribute to damage and collapse. Contributions of Chapter 4 are prediction of damage and collapse as a function of hurricane hazards, building attributes, and their interactions; identification of the hazard and building variables that significantly contribute to damage and collapse; interpretation of the manner in which the hazard-

damage relationship significantly differs given levels of building attributes; and validation of model prediction accuracy.

5.5 Final Remarks and Recommendations

The overarching goal of this dissertation was to improve data-based damage prediction for residential construction subjected to multi-hazard hurricane hazards at the individual building scale. This was accomplished primarily through the development of two model types. The first model type predicts building damage as a function of hazard parameters, and the second model type predicts damage as a function of hazard parameters, building attributes, and their interactions. Additionally, to maximize use of aftermath datasets with missing building attribute data, diagnostic and comparison approaches were developed to evaluate the performance of binary variable imputation models. The preceding sections describe the work accomplished to develop the two models and the diagnostic and comparison approaches.

In the future, more comprehensive models can be developed by considering more building attributes (e.g., cladding type, roof shape, age), environmental attributes (e.g., soil type, spacing between buildings), and interaction terms (e.g. HE, HHE, HHA, HHHA, HHHE). Application of the models on such comprehensive data from other events (e.g., Hurricanes Sandy and Harvey) and regions will confirm the effectiveness of the developed predictive models for predicting damage and identifying hazard and building attribute variables that significantly contribute to damage and collapse.

For those involved in damage modeling, the results of this research point to the hazard and building attribute variables that are significant predictors of damage and collapse. Therefore, this work can serve as a starting point for future data-based and analytical models. The use of the seven-category WF damage scale and the application of dependent variable aggregation are a significant contribution that provides flexibility for modeling the response variable. Finally, while data-based

hurricane fragility modeling is a relatively newer field of study, all published papers suffer from the same general deficiencies. The methods developed in this dissertation directly address these deficiencies and are intended to make significant theoretical contributions to the field of data-based fragility modeling.

5.6 Study Limitations

The study is limited to one- and two-story wood-framed single family homes with slab and elevated foundations subjected to hurricane hazards. The dataset used to develop the fragility model is limited to data resulting from rapid damage assessment using the recorded video approach after 2005 Hurricane Katrina. The proposed fragility model describes damage in accordance with the WF Damage Scale (Friedland and Levitan, 2009), which does not explicitly consider interior damage. While the damage reconnaissance included multiple communities with increasing distance from the hurricane track, and thus decreasing hazard levels, the maximum 3-second gust wind speeds ranged between 48 and 68 m/s. Wind damage was limited during Hurricane Katrina due to these lower wind speeds. (Masters et al., 2009) report that roof cover damage typically starts at peak gust wind speeds of 31 to 36 m/s and (van de Lindt et al., 2007) observed frequent loss of roof cover in a Hurricane Katrina reconnaissance. However, because pressure is proportional to the square of the wind speed, the wind speeds experienced in Hurricane Katrina did not cause substantial damage, which limits the applicability of this model to more intense wind events. The fragility models have been developed and validated only within the ranges of hazards experienced in Hurricane Katrina and for the building attributes and practices used in coastal Mississippi. A limitation of the underlying building and damage data is that a specified sampling technique was not implemented during the original field data collection and required sample sizes in each DS were not considered. Although the fragility models are developed for certain hazards and structure types, the underlying development of the methodology for developing and validating the fragility

model is applicable to other hazards (e.g., flood, earthquake, fire) and building types (e.g. commercial). Although the application of the developed diagnostic and comparison approaches is for binary variable with missing observations, the methodology is applicable to other variable (e.g. multinomial) and other imputation technique (e.g., predictive mean matching for multinomial variable).

REFERENCES

Abayomi, K., Gelman, A., & Levy, M. (2008). Diagnostics for multivariate imputations. *Journal of the Royal Statistical Society: Series C (Applied Statistics), 57*(3), 273-291. doi: http://doi.org/10.1111/j.1467-9876.2007.00613.x

Adams, B. J., Huyck, C., Mio, M., Cho, S., Eguchi, R. T., Womble, A., & Mehta, K. (2004). *Streamlining post-disaster data collection and damage assessment, using VIEWS (visualizing impacts of earthquakes with satellites) and VRS (virtual reconnaissance system).* Paper presented at the Proceedings of 2nd International Workshop on Remote Sensing for Post-Disaster Response, Newport Beach, California.

Akande, O., Li, F., & Reiter, J. (2017). An empirical comparison of multiple imputation methods for categorical data. *The American Statistician, 71*(2), 162-170. doi: http://doi.org/10.1080/00031305.2016.1277158

American Society of Civil Engineers (ASCE). (2010). Minimum design loads for buildings and other structures. Reston, VA: American Society of Civil Engineers.

Baradaranshoraka, M., Pinelli, J.-P., Gurley, K., Peng, X., & Zhao, M. (2017). Hurricane wind versus storm surge damage in the context of a risk prediction model. *Journal of Structural Engineering, 143*(9). doi: http://doi.org/10.1061/(ASCE)ST.1943-541X.0001824

Barbato, M., Petrini, F., Unnikrishnan, V. U., & Ciampoli, M. (2013). Performance-based hurricane engineering (PBHE) framework. *Structural Safety, 45*, 24-35. doi: http://10.1016/j.strusafe.2013.07.002

Berglund, P., & Heeringa, S. G. (2014). *Multiple imputation of missing data using SAS*. Cary, NC: SAS Institute.

Bernhardt, P. W. (2018). Model validation and influence diagnostics for regression models with missing covariates. *Statistics in Medicine, 37*(8), 1325-1342. doi: https://doi.org/10.1002/sim.7584

Booij, N., Ris, R., & Holthuijsen, L. H. (1999). A third-generation wave model for coastal regions: 1. Model description and validation. *Journal of Geophysical Research: Oceans, 104*(C4), 7649-7666. doi: http://10.1029/98JC02622

Bunya, S., Dietrich, J. C., Westerink, J., Ebersole, B., Smith, J., Atkinson, J., Jensen, R., Resio, D., Luettich, R., & Dawson, C. (2010). A high-resolution coupled riverine flow, tide, wind,

wind wave, and storm surge model for southern Louisiana and Mississippi. Part I: Model development and validation. *Monthly Weather Review, 138*(2), 345-377. doi: http://doi.org/10.1175/2009MWR2906.1

Cabras, S., Castellanos, M. E., & Quirós, A. (2011). Goodness-of-fit of conditional regression models for multiple imputation. *Bayesian Analysis, 6*(3), 429-455. doi: http://doi.org/10.1214/11-BA617

Cardone, V., & Cox, A. (2009). Tropical cyclone wind field forcing for surge models: critical issues and sensitivities. *Natural Hazards, 51*(1), 29-47. doi: http://doi.org/10.1007/s11069-009-9369-0

Charvet, I., Ioannou, I., Rossetto, T., Suppasri, A., & Imamura, F. (2014a). Empirical fragility assessment of buildings affected by the 2011 Great East Japan tsunami using improved statistical models. *Natural Hazards, 73*(2), 951-973. doi: http://doi.org/10.1007/s11069-014-1118-3

Charvet, I., Suppasri, A., & Imamura, F. (2014b). Empirical fragility analysis of building damage caused by the 2011 Great East Japan tsunami in Ishinomaki city using ordinal regression, and influence of key geographical features. *Stochastic Environmental Research and Risk Assessment, 28*(7), 1853-1867. doi: https://doi.org/10.1007/s00477-014-0850-2

Charvet, I., Suppasri, A., Kimura, H., Sugawara, D., & Imamura, F. (2015). A multivariate generalized linear tsunami fragility model for Kesennuma City based on maximum flow depths, velocities and debris impact, with evaluation of predictive accuracy. *Natural Hazards, 79*(3), 2073-2099. doi: https://doi.org/10.1007/s11069-015-1947-8

Choine, M. N., O'Connor, A., Gehl, P., D'Ayala, D., García-Fernández, M., Jiménez, M.-J., Gavin, K., Van Gelder, P., Salceda, T., & Power, R. (2015). *A multi hazard risk assessment methodology accounting for cascading hazard events.* Paper presented at the Proceedings of 12th International Conference on Applications of Statistics and Probability in Civil Engineering (ICASP12), Vancouver, Canada.

Collins, L. M., Schafer, J. L., & Kam, C.-M. (2001). A comparison of inclusive and restrictive strategies in modern missing data procedures. *Psychological Methods, 6*(4), 330. doi: http://dx.doi.org/10.1037/1082-989X.6.4.330

Cox, A., Greenwood, J., Cardone, V., & Swail, V. (1995). *An interactive objective kinematic analysis system.* Paper presented at the Proceedings of Fourth International Workshop on Wave Hindcasting and Forecasting.

Dietrich, J. C., Bunya, S., Westerink, J., Ebersole, B., Smith, J., Atkinson, J., Jensen, R., Resio, D., Luettich, R., & Dawson, C. (2010). A high-resolution coupled riverine flow, tide, wind, wind wave, and storm surge model for southern Louisiana and Mississippi. Part II: Synoptic description and analysis of Hurricanes Katrina and Rita. *Monthly Weather Review, 138*(2), 378-404. doi: http://doi.org/10.1175/2009MWR2907.1

Dietrich, J. C., Tanaka, S., Westerink, J. J., Dawson, C., Luettich Jr, R., Zijlema, M., Holthuijsen, L. H., Smith, J., Westerink, L., & Westerink, H. (2012). Performance of the unstructured-mesh, SWAN+ ADCIRC model in computing hurricane waves and surge. *Journal of Scientific Computing, 52*(2), 468-497. doi: http://doi.org/10.1007/s10915-011-9555-6

Durst, C. (1960). Wind speeds over short periods of time. *Meteorological Magazine, 89*, 181-186.

Ellingwood, B. R., Rosowsky, D. V., Li, Y., & Kim, J. H. (2004). Fragility assessment of light-frame wood construction subjected to wind and earthquake hazards. *Journal of Structural Engineering, 130*(12), 1921-1930. doi: http://doi.org/10.1061/(ASCE)0733-9445

Farhan, J., & Fwa, T. (2014). Improved imputation of missing pavement performance data using auxiliary variables. *Journal of Transportation Engineering, 141*(1), 04014-04065. doi: https://doi.org/10.1061/(ASCE)TE.1943-5436.0000725

Fay, R. E. (1996). Alternative paradigms for the analysis of imputed survey data. *Journal of the American Statistical Association, 91*(434), 490-498. doi: http://doi.org/10.2307/2291636

Ferrari, P. A., Annoni, P., Barbiero, A., & Manzi, G. (2011). An imputation method for categorical variables with application to nonlinear principal component analysis. *Computational Statistics & Data Analysis, 55*(7), 2410-2420. doi: https://doi.org/10.1016/j.csda.2011.02.007

Friedland, C. J., & Gall, M. (2012). True cost of hurricanes: Case for a comprehensive understanding of multihazard building damage. *Leadership and Management in Engineering, 12*(3), 134-146. doi: https://doi.org/10.1061/(ASCE)LM.1943-5630.0000178

Friedland, C. J., & Levitan, M. L. (2009). *Loss-consistent categorization of hurricane wind and storm surge damage for residential structures.* Paper presented at the Proceedings of the 11th Americas Conference on Wind Engineering, San Juan, Puerto Rico.

Fritz, H. M., Blount, C., Sokoloski, R., Singleton, J., Fuggle, A., McAdoo, B. G., Moore, A., Grass, C., & Tate, B. (2008). Hurricane Katrina storm surge reconnaissance. *Journal of*

Geotechnical and Geoenvironmental Engineering, 134(5), 644-656. doi: https://doi.org/10.1061/(ASCE)1090-0241(2008)134:5(644)

Geisser, S. (1975). The predictive sample reuse method with applications. *Journal of the American Statistical Association, 70*(350), 320-328. doi: https://doi.org/10.2307/2285815

Gelman, A., Van Mechelen, I., Verbeke, G., Heitjan, D. F., & Meulders, M. (2005). Multiple imputation for model checking: Completed-data plots with missing and latent data. *Biometrics, 61*(1), 74-85. doi: https://doi.org/10.1111/j.0006-341X.2005.031010.x

Grayson, M. J., Pang, W., & Schiff, S. (2013). Building envelope failure assessment framework for residential communities subjected to hurricanes. *Engineering Structures, 51*(0), 245-258. doi: http://dx.doi.org/10.1016/j.engstruct.2013.01.027

Hatzikyriakou, A. (2017). *Vulnerability and hazard modeling for coastal flooding due to storm surge*. (PhD Dissertation), Princeton University, Princeton, New Jersey.

Hatzikyriakou, A., & Lin, N. (2018). Assessing the vulnerability of structures and residential communities to storm surge: An analysis of flood impact during Hurricane Sandy. *Frontiers in Built Environment, 4*(4). doi: https://doi.org/10.3389/fbuil.2018.00004

Hatzikyriakou, A., Lin, N., Gong, J., Xian, S., Hu, X., & Kennedy, A. (2015). Component-based vulnerability analysis for residential structures subjected to storm surge impact from Hurricane Sandy. *Natural Hazards Review, 17*(1). doi: https://doi.org/10.1061/(ASCE)NH.1527-6996.0000205

Jaccard, J., & Turrisi, R. (2003). *Interaction effects in multiple regression*. Newbury Park, Calif: Sage.

Kalnay, E., Kanamitsu, M., Kistler, R., Collins, W., Deaven, D., Gandin, L., Iredell, M., Saha, S., White, G., & Woollen, J. (1996). The NCEP/NCAR 40-year reanalysis project. *Bulletin of the American Meteorological Society, 77*(3), 437-471. doi: https://doi.org/10.1175/1520-0477(1996)077<0437:TNYRP>2.0.CO;2

Kameshwar, S., & Padgett, J. E. (2018). Fragility and resilience indicators for portfolio of oil storage tanks subjected to hurricanes. *Journal of Infrastructure Systems, 24*(2), 04018003. doi: https://doi.org/10.1061/(ASCE)IS.1943-555X.0000418

Kappes, M., Keiler, M., von Elverfeldt, K., & Glade, T. (2012a). Challenges of analyzing multi-hazard risk: A review. *Natural Hazards, 64*(2), 1925-1958. doi: http://doi.org/10.1007/s11069-012-0294-2

Kappes, M. S., Papathoma-Köhle, M., & Keiler, M. (2012b). Assessing physical vulnerability for multi-hazards using an indicator-based methodology. *Applied Geography, 32*(2), 577-590. doi: https://doi.org/10.1016/j.apgeog.2011.07.002

Katz, R. W. (2013). *Economic impact of extreme events: An approach based on extreme value theory*. Washington, DC: Wiley.

Kennedy, A., Rogers, S., Sallenger, A., Gravois, U., Zachry, B., Dosa, M., & Zarama, F. (2010). Building destruction from waves and surge on the Bolivar Peninsula during Hurricane Ike. *Journal of Waterway, Port, Coastal, and Ocean Engineering, 137*(3), 132-141. doi: https://doi.org/10.1061/(ASCE)WW.1943-5460.0000061

Krayer, W. R., & Marshall, R. D. (1992). Gust factors applied to hurricane winds. *Bulletin of the American Meteorological Society, 73*(5), 613-618. doi: https://doi.org/10.1175/1520-0477(1992)073<0613:GFATHW>2.0.CO;2

Lallemant, D., Kiremidjian, A., & Burton, H. (2015). Statistical procedures for developing earthquake damage fragility curves. *Earthquake Engineering & Structural Dynamics*. doi: https://doi.org/10.1002/eqe.2522

Lee, K. H., & Rosowsky, D. V. (2006). Fragility analysis of woodframe buildings considering combined snow and earthquake loading. *Structural Safety, 28*(3), 289-303. doi: http://doi.org/10.1016/j.strusafe.2005.08.002

Li, Y., & Ellingwood, B. R. (2009a). Framework for multihazard risk assessment and mitigation for wood-frame residential construction. *Journal of Structural Engineering, 135*(2), 159-168. doi: https://doi.org/10.1061/(ASCE)0733-9445(2009)135:2(159)

Li, Y., & Ellingwood, B. R. (2009b). Risk-based decision-making for multi-hazard mitigation for wood-frame residential construction. *Australian Journal of Structural Engineering, 9*(1), 17. doi: https://doi.org/10.1080/13287982.2009.11465006

Li, Y., & van de Lindt, J. W. (2012). Loss-based formulation for multiple hazards with application to residential buildings. *Engineering Structures, 38*(0), 123-133. doi: https://doi.org/10.1016/j.engstruct.2012.01.006

Li, Y., van de Lindt, J. W., Dao, T., Bjarnadottir, S., & Ahuja, A. (2011). Loss analysis for combined wind and surge in hurricanes. *Natural Hazards Review, 13*(1), 1-10. doi: https://doi.org/10.1061/(ASCE)NH.1527-6996.0000058

Lillesand, T., Kiefer, R. W., & Chipman, J. (2014). *Remote Sensing and Image Interpretation*. New York: John Wiley & Sons.

Liu, Z., Nadim, F., Garcia-Aristizabal, A., Mignan, A., Fleming, K., & Luna, B. Q. (2015). A three-level framework for multi-risk assessment. *Georisk: Assessment and Management of Risk for Engineered Systems and Geohazards, 9*(2), 59-74. doi: https://doi.org/10.1080/17499518.2015.1041989

Luettich, R. A., & Westerink, J. J. (2004). Formulation and numerical implementation of the 2D/3D ADCIRC finite element model version 44. XX. Retrieved from https://adcirc.org/adcirc_theory_2004_12_08.pdf

Marzocchi, W., Garcia-Aristizabal, A., Gasparini, P., Mastellone, M. L., & Di Ruocco, A. (2012). Basic principles of multi-risk assessment: A case study in Italy. *Natural Hazards, 62*(2), 551-573. doi: https://doi.org/10.1007/s11069-012-0092-x

Masters, F., Vickery, P., Harper, B., Powell, M., & Reinhold, T. (2009). *Engineering guidance regarding wind-caused damage descriptors*.

McCullough, M. C., Kareem, A., Donahue, A. S., & Westerink, J. J. (2013). Structural damage under multiple hazards in coastal environments. *Journal of Disaster Research, 8*, 1042-1051. doi: https://doi.org/10.20965/jdr.2013.p1042

Meng, X.-L. (1994). Multiple-imputation inferences with uncongenial sources of input. *Statistical Science, 9*(4), 538-558. doi: https://doi.org/10.1214/ss/1177010270

Nateghi, R., Guikema, S. D., & Quiring, S. M. (2011). Comparison and validation of statistical methods for predicting power outage durations in the event of hurricanes. *Risk Analysis: An International Journal, 31*(12), 1897-1906. doi: https://doi.org/10.1111/j.1539-6924.2011.01618.x

Nguyen, C. D., Carlin, J. B., & Lee, K. J. (2017). Model checking in multiple imputation: An overview and case study. *Emerging Themes in Epidemiology, 14*(1), 8. doi: https://doi.org/10.1186/s12982-017-0062-6

NIST National Institute of Standards and Technology. (2011). Disaster and Failure Studies Data Repository. https://www.nist.gov/topics/disaster-failure-studies/disaster-failure-studies-data-repository

Pan, F. (2014). *Damage prediction of low-rise buildings under hurricane winds.* (PhD Dissertation), Louisiana State University, Baton Rouge, LA.

PEER Pacific Earthquake Engineering Research Center. (2011). PEER Ground Motion Database. http://peer.berkeley.edu/

Pitilakis, K., Crowley, H., & Kaynia, A. (2014). *SYNER-G: Typology definition and fragility functions for physical elements at seismic risk* (Vol. 27). Netherlands: Springer

Powell, M. D., & Houston, S. H. (1996). Hurricane Andrew's landfall in South Florida. Part II: Surface wind fields and potential real-time applications. *Weather and Forecasting, 11*(3), 329-349. doi: https://doi.org/10.1175/1520-0434(1996)011<0329:HALISF>2.0.CO;2

Powell, M. D., Houston, S. H., Amat, L. R., & Morisseau-Leroy, N. (1998). The HRD real-time hurricane wind analysis system. *Journal of Wind Engineering and Industrial Aerodynamics, 77*, 53-64. doi: https://doi.org/10.1016/S0167-6105(98)00131-7

Powell, M. D., Houston, S. H., & Reinhold, T. A. (1996). Hurricane Andrew's landfall in south Florida. Part I: Standardizing measurements for documentation of surface wind fields. *Weather and Forecasting, 11*(3), 304-328.

Raghunathan, T. E., Lepkowski, J. M., Van Hoewyk, J., & Solenberger, P. (2001). A multivariate technique for multiply imputing missing values using a sequence of regression models. *Survey Methodology, 27*(1), 85-96. doi: http://10.1.1.405.4540

Reed, D. A., Friedland, C. J., Wang, S., & Massarra, C. C. (2016). Multi-hazard system-level logit fragility functions. *Engineering Structures, 122*, 14-23. doi: http://dx.doi.org/10.1016/j.engstruct.2016.05.006

Reese, S., Bradley, B. A., Bind, J., Smart, G., Power, W., & Sturman, J. (2011). Empirical building fragilities from observed damage in the 2009 South Pacific Tsunami. *Earth-Science Reviews, 107*(1), 156-173. doi: https://doi.org/10.1016/j.earscirev.2011.01.009

Rubin, D. B. (1978). *Multiple imputations in sample surveys-a phenomenological Bayesian approach to nonresponse.* Paper presented at the Proceedings of the survey research methods section of the American Statistical Association.

Schmidt, J., Matcham, I., Reese, S., King, A., Bell, R., Henderson, R., Smart, G., Cousins, J., Smith, W., & Heron, D. (2011). Quantitative multi-risk analysis for natural hazards: A framework for multi-risk modelling. *Natural Hazards, 58*(3), 1169-1192. doi: http://doi.org/10.1007/s11069-011-9721-z

Schomaker, M., & Heumann, C. (2014). Model selection and model averaging after multiple imputation. *Computational Statistics & Data Analysis, 71*(Supplement C), 758-770. doi: https://doi.org/10.1016/j.csda.2013.02.017

Stone, M. (1974). Cross-validatory choice and assessment of statistical predictions. *Journal of the Royal Statistical Society. Series B (Methodological)*, 111-147.

Stuart, E. A., Azur, M., Frangakis, C., & Leaf, P. (2009). Multiple imputation with large data sets: A case study of the Children's Mental Health Initiative. *American Journal of Epidemiology, 169*(9), 1133-1139. doi: https://doi.org/10.1093/aje/kwp026

Tomiczek, T., Kennedy, A., & Rogers, S. (2014a). Collapse limit state fragilities of wood-framed residences from storm surge and waves during Hurricane Ike. *Journal of Waterway, Port, Coastal, and Ocean Engineering, 140*(1), 43-55. doi: https://doi.org/10.1061/(ASCE)WW.1943-5460.0000212

Tomiczek, T., Kennedy, A., & Rogers, S. (2014b). Survival analysis of elevated homes on the Bolivar Peninsula after Hurricane Ike. *Bridges, 10*, 108-118. doi: https://doi.org/10.1061/9780784412626.010

Tomiczek, T., Kennedy, A., Zhang, Y., Owensby, M., Hope, M. E., Lin, N., & Flory, A. (2017). Hurricane damage classification methodology and fragility functions derived from Hurricane Sandy's effects in coastal New Jersey. *Journal of Waterway, Port, Coastal, and Ocean Engineering, 143*(5). doi: https://doi.org/10.1061/(ASCE)WW.1943-5460.0000409

Van Buuren, S. (2012). *Flexible imputation of missing data*. New York: CRC Press.

van de Lindt, J. W., Graettinger, A., Gupta, R., Skaggs, T., Pryor, S., & Fridley, K. J. (2007). Performance of wood-frame structures during Hurricane Katrina. *Journal of Performance of Constructed Facilities, 21*(2), 108-116. doi: https://doi.org/10.1061/(ASCE)0887-3828(2007)21:2(108)

van Verseveld, H. C. W., van Dongeren, A. R., Plant, N. G., Jäger, W. S., & den Heijer, C. (2015). Modelling multi-hazard hurricane damages on an urbanized coast with a Bayesian network approach. *Coastal Engineering, 103*(0), 1-14. doi: http://doi.org/10.1016/j.coastaleng.2015.05.006

Vickery, P., & Twisdale, L. (1995). Wind-field and filling models for hurricane wind-speed predictions. *Journal of Structural Engineering, 121*(11), 1700-1709. doi: https://doi.org/10.1061/(ASCE)0733-9445(1995)121:11(1700)

Vickery, P. J., Skerlj, P., Steckley, A., & Twisdale, L. (2000). Hurricane wind field model for use in hurricane simulations. *Journal of Structural Engineering, 126*(10), 1203-1221. doi: https://doi.org/10.1061/(ASCE)0733-9445(2000)126:10(1203)

Westerink, J. J., Luettich, R. A., Feyen, J. C., Atkinson, J. H., Dawson, C., Roberts, H. J., Powell, M. D., Dunion, J. P., Kubatko, E. J., & Pourtaheri, H. (2008). A basin-to channel-scale unstructured grid hurricane storm surge model applied to southern Louisiana. *Monthly Weather Review, 136*(3), 833-864. doi: https://doi.org/10.1175/2007MWR1946.1

White, I. R., Royston, P., & Wood, A. M. (2011). Multiple imputation using chained equations: Issues and guidance for practice. *Statistics in Medicine, 30*(4), 377-399. doi: https://doi.org/10.1002/sim.4067

Zhang, Y., Kennedy, A. B., Tomiczek, T., Yang, W., Liu, W., & Westerink, J. J. (2017). Assessment of hydrodynamic competence in extreme marine events through application of Boussinesq–Green–Naghdi models. *Applied Ocean Research, 67*, 136-147. doi: https://doi.org/10.1016/j.apor.2017.06.001

Zhu, H., Ibrahim, J. G., & Shi, X. (2009). Diagnostic measures for generalized linear models with missing covariates. *Scandinavian Journal of Statistics, 36*(4), 686-712. doi: http://doi.org/10.1111/j.1467-9469.2009.00644.x

APPENDIX A. COMPUTATIONALLY MODELED EXPLANATORY HAZARD VARIBLES

Hazard attributes were characterized via a coupled modeling system for hurricane winds, waves, and storm surge (Bunya et al., 2010; Dietrich et al., 2010). This system represents the coastal environment with varying levels of resolution to predict the storm-induced development of waves and surge in open water and then their interactions with fine-scale coastal features. The model results were then interpolated spatially to provide time series at the building locations.

The wind field for Katrina was developed from analyses of airborne and land-based observations, which were assimilated and transformed to a common reference condition for the inner core by using the NOAA Hurricane Research Division Wind Analysis System (H*WIND) (Powell et al., 1998; Powell et al., 1996). These winds were then blended with peripheral winds from the National Centers for Environmental Prediction – National Center for Atmospheric Research (NCEP-NCAR) reanalysis project (Kalnay et al., 1996), by using the Interactive Objective Kinematic Analysis (IOKA) system (Cardone & Cox, 2009; Cox et al., 1995) The resulting wind fields provide coverage of the entire Gulf of Mexico on a regular grid with snapshots every 15 min.

These wind fields were then interpolated spatially and temporally for use by the coupled SWAN+ADCIRC (Westerink et al., 2008) models. SWAN represents the wave field as a phase-averaged spectrum (Booij et al., 1999). The wave action density $N(t, \lambda, \varphi, \sigma, \theta)$ evolves in time (t), geographic space (with longitudes λ and latitudes φ) and spectral space (with relative frequencies σ and directions θ), as governed by the action balance equation. Source terms represent wave growth by wind; energy lost due to whitecapping, depth-induced breaking, and bottom friction; and energy exchanged between spectral components due to nonlinear effects in deep and shallow water. Wave refraction and frequency shifting are represented via coupling with ADCIRC,

which solves modified forms of the shallow-water equations for water levels ζ and depth-averaged currents U and V (Luettich & Westerink, 2004; Westerink et al., 2008). These models are coupled tightly so information is passed through local memory, efficient on high-performance computing systems, and validated for hurricane wave and flooding applications along the U. S. Atlantic and Gulf coastlines (Dietrich et al., 2012).

SWAN+ADCIRC uses unstructured meshes containing triangular finite elements of varying sizes, ranging from kilometers in open water, to hundreds of meters near the coastline and through the floodplains, and to tens of meters in the small-scale natural and man-made channels that convey surge into inland regions. It is noted that SWAN+ADCIRC does not represent the interactions of built infrastructure with storm-driven waves and currents, but rather it represents their effects with bulk parameterizations including wind reduction due to overland roughness and canopy, and bottom friction due to land cover. Thus the computed waves and surge may not represent the fine-scale set-up and dissipation caused by individual structures. However, the SWAN+ADCIRC simulations are valuable because they cover large portions of the coast (including communities with devastation that may not be known a priori) and become available even during the storm events due to real-time forecasting. Katrina was simulated on the SL16 mesh (Dietrich et al., 2012).

At the building locations shown in Figure 1, hazard attributes were interpolated spatially to provide time series of:

- Wind speed (U_{10}; m/s), provided at an elevation of 10 m and with an averaging period of 10 min, and used as forcing to the wave and surge models;
- Significant wave height (H_S; m), which is a statistical property computed by integrating the action density in spectral space in SWAN;

- Water level (ζ; m relative to NAVD88), computed by ADCIRC and representing the combined contributions of tides, storm surge, and wave-induced setup; and
- Water speed (*U*; m/s), computed by ADCIRC and representing the depth-averaged flow at each location.

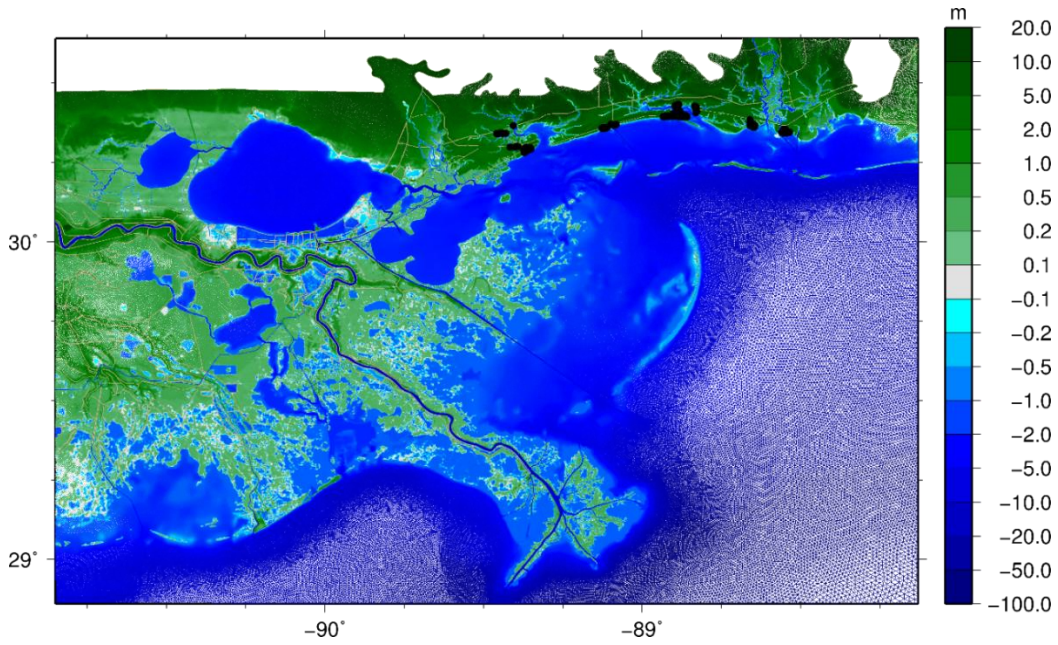

Figure A.1 Bathymetry / topography (m) of the SL16 mesh in southeastern Louisiana; the mesh extends throughout the Gulf of Mexico and the western North Atlantic Ocean (Dietrich et al., 2012). Building locations for the analyses are shown in black dots.

The maximum value for each variable at each building location was extracted and used to represent maximum 3-second gust wind speed, $U_{3.\max}$; maximum significant wave height, $H_{S,max}$; maximum surge depth above local ground, D_{max}; and maximum water speed, U_{max}.

VITA

Carol C. Massarra was born in Lattakia, Syria. She earned a bachelor's degree in civil engineering (B.C.E.) from Tishreen University, Lattakia, Syria, in 1999. Upon graduation, Carol worked as an instructor in the Faculty of Civil Engineering at Tishreen University from 1999 until 2009. She earned a master of science (M.S.) in engineering science from Louisiana State University (LSU) in August 2012 and a master of applied statistics (M.Ap.Stat.) from LSU in August 2016. Carol has held multiple research fellowships at LSU and is the instructor of record for the construction management capstone course in the Bert S. Turner Department of Construction Management at LSU.